United States Department of Commerce
Technology Administration
National Institute of Standards and Technology

NIST Technical Note 1382

A Standard Source Method for Reducing Antenna Factor Errors in Shielded Room Measurements

Dennis Camell
Galen Koepke
Robert Smith
Bob Rakoski

TN 1382

A Standard Source Method for Reducing Antenna Factor Errors in Shielded Room Measurements

Dennis Camell
Galen Koepke
Robert Smith
Bob Rakoski

Electromagnetic Fields Division
Electronics and Electrical Engineering Laboratory
National Institute of Standards and Technology
325 Broadway
Boulder, Colorado 80303-3328

March 1996

U.S. DEPARTMENT OF COMMERCE, Ronald H. Brown, Secretary
TECHNOLOGY ADMINISTRATION, Mary L. Good, Under Secretary for Technology
NATIONAL INSTITUTE OF STANDARDS AND TECHNOLOGY, Arati Prabhakar, Director

National Institute of Standards and Technology Technical Note
Natl. Inst. Stand. Technol., Tech. Note 1382, 44 pages (March 1996)
CODEN:NTNOEF

U.S. GOVERNMENT PRINTING OFFICE
WASHINGTON: 1996

For sale by the Superintendent of Documents, U.S. Government Printing Office, Washington, DC 20402-9325

CONTENTS

A Standard Source Method for Reducing Antenna Factor Errors in Shielded Room Measurements

Dennis Camell and Galen Koepke
National Institute of Standards and Technology
Boulder, CO 80303
and
Robert Smith and Bob Rakoski
Eagle Systems, Inc.
California, MD 20619

In this report we will examine the use of a well characterized standard source of electromagnetic radiation as a means to calibrate the effects of the shielded room on a receiving antenna used for MILSTD 461/462 RE102 emissions measurement. The goal was to compensate for the shielded room environment so that radiated emissions measurements can be more accurately compared from one room to another. This was accomplished by using a characterized spherical dipole source to calibrate an antenna's response in the location that it was used. An interlaboratory comparison was made of the detected emissions from a simulated equipment-under-test at three sites to see how this in-situ calibration of the receive antenna helped the shielded room test repeatability.

Key words : antenna factor, intercomparison, shielded room, spherical dipole, standard source.

1. Introduction

The shielded (or screened) room continues to be widely used as a facility to measure electromagnetic emissions and susceptibility of electronic systems even though the technical difficulties are well documented [1-7] and can lead to large measurement errors. The appeal of shielded room measurements is a combination of economics, inertia (they have been used for decades), problems or limitations in other techniques, and the fact that performance/procurement standards such as MILSTD 461/462 specify using shielded rooms [8,9]. To their credit, shielded rooms are relatively inexpensive, provide isolation from the external environment, protect the security or confidentiality of the test item, and are used at some frequencies where there is not a good substitute technique.

The reality of this situation has motivated researchers to investigate techniques for reducing errors in shielded room measurements. Some of the suggested improvements have included hooded antennas [3,10], electrically small probes [10,11], alternative procedures for specific situations [12,13], development of numerical and circuit modeling tools to help explain measurement results [14-16], the use of electromagnetic absorbing material to reduce room reflections [11,17,18], and development of antenna-shielded room calibration procedures [19-21].

The experimental work we present in this report explores the concept of a antenna-in-shielded room calibration procedure. The antenna factor (AF) of an antenna, as the ratio of the antenna's response to the transmitted signal, depends upon the environment of the test. The test environment within a shielded room highly depends upon the placement of the objects (antennas included) in the room, as detailed in section 2. Therefore, to obtain accurate AF data for the antenna, it should be measured in the environment that it is used. This procedure is similar to that proposed by Marvin, et al. [19-21]. We have applied this concept to an electric dipole source and simple test items over the frequency range of 30 MHz to 1 GHz. We performed these experiments at three different laboratories to study the issue of repeatability between several different shielded rooms.

This technical note is organized as follows: Section 2 provides some background information on shielded rooms and Section 3 on the spherical dipole source. Section 4 explains the calibration procedures used to quantify the emission from the spherical dipole in free-field environments like the anechoic chamber and open area test site. This calibration will be used as a reference to determine emissions in the shielded room. A bridge is needed between the open area test site (OATS) and anechoic chamber environments to the shielded room environment; section 5 presents measurements relating the two environments using the spherical dipole source. We discuss the technique for calibrating the source-shielded room-receiving antenna configuration and related details in section 6. Also in section 6, we deal with the data accumulated at three different MILSTD 461/462 laboratories. The data include a repeat of earlier work at these laboratories, which examined variations and results using conventional procedures [6,7]. Finally, we summarize our observations and recommendations in section 7, and list the references in section 8.

2. Shielded Room Emissions Measurements - An Overview

A comprehensive treatment of the problems that are encountered in performing shielded room measurements is beyond the scope of this report, but a few comments are useful as background. There are several reasons for potentially large errors in electromagnetic interference/compatibility (EMI/EMC) measurements performed in a shielded room. Perhaps the most obvious is the fact that the shielded room is a conducting cavity and thus it exhibits cavity resonances, standing waves, and, at lower frequencies, evanescent waveguide modes [19]. The fields produced by a source in this highly reflective environment have been shown to vary by as much as ±40 dB [2,4] throughout the measurement volume. This lack of field uniformity means that the measured field strength is sensitive to the measurement geometry. This measurement geometry is the positions of the source and antenna(s), the size and shape of the room, and locations of other conducting objects in the room.

Another potential source of error is that the characteristics of the receiving antenna can be altered by the proximity of the conducting surfaces. The interactions of the antenna and its many images will cause its AF, and consequently the antenna's response to the field, to be sensitive to the measurement geometry. This can cause the AF to be significantly different than the free-space value at certain frequencies. The equipment-under-test (EUT) can also be thought of as an antenna (unintentional perhaps) that is affected by the room in a similar manner; and thus the radiation characteristics can change depending on the geometry and may be different when compared to OATS or anechoic chambers. A third complication in shielded rooms is that the coupling mechanism for energy transfer from source (or EUT) to receiving antenna is more complicated than in a free field environment [19]. This is due to the conducting surfaces of the room and the fact that the EUT and receiving antenna are in the near field of each other.

The preceding paragraph may lead one to conclude that repeatable shielded room measurements are nearly impossible. This is certainly not the attitude of the MILSTD 461/462 measurement community, for whom shielded rooms continue to be the primary facility for EMI/EMC radiated testing. The authors of the latest revision of MILSTD 461/462, revision D (1993) [8,9], were aware of the challenges imposed by the shielded room environment. This document includes at least three important methods for controlling the repeatability of measurements. The first is common to most documents of this type, and that is to control the geometry by clearly specifying every component and dimension involved in the test. This is necessary considering the nature of the shielded room environment and the purpose of the testing. However, it is not sufficient in light of the fact that rooms can vary in size and shape and that, within a single unloaded room, changing position of an antenna by only 2 cm (well within the positioning tolerance specified) can result in response variations of up to 15 dB or more [4].

The next logical refinement then is to dampen the electromagnetic fields in the room so that the positioning specifications are practical. These documents [8,9] acknowledge the benefits of electromagnetic absorbing material and includes a considerable amount in the room specifications. This can be very beneficial at frequencies where the absorbing material is effective (consider an anechoic chamber) but loses its value at the lower frequencies. These lower frequency measurements should improve as more effective absorbing materials become available and are installed in these chambers.

The last point in this discussion is the requirement for calibration of the measurement system and antennas. It is good engineering practice to maintain the calibration of every component in the system, including antennas. Revision D of MILSTD 461/462 refers to SAE ARP-958 [22] for the calibration of antenna factors but does not include a requirement that the calibration be performed in the same configuration and location in the shielded room where the antenna will be used. In this report we will concentrate on the effects of various antenna calibration techniques (vendor supplied, at the open area test site, and in the shielded room) and quantify any possible benefits of calibrating the antenna and shielded room as one unit.

3. A Standard Source

One of the first requirements for evaluating electromagnetic emission measurements is to have a source which can be completely characterized, preferably by analytical and/or empirical methods which are independent of the technique being evaluated. The source must also remain constant and be insensitive to the test environment. An example of such a source is a small (10 cm diameter) spherical dipole. This type of source has been used successfully for some time [23], and recently NIST has developed a new version making extensive use of optical fiber technology [24]. This design, which will be described shortly, is now available commercially. A similar spherical dipole has also been used successfully by researchers in England [18,20,21] to look at emissions from both electric and magnetic dipoles in shielded enclosures. According to Marvin, et al. [20], the spherical dipole, which possesses electric dipole moments, can be converted to a magnetic dipole by the addition of a conducting loop between the two poles of the sphere. However, a complete examination of both source types was not the scope of this study; all the measurements presented in this report are for an electric dipole source.

The spherical dipole radiator used in this study is described in detail in Ref. [24]. A brief description of the principal features would be useful to help understand the measurements discussed later. The radiating element is a gold-plated, spherical dipole with diameter of 10 cm and a 3 mm gap on the equator. All signals to and from the sphere are transmitted by optical fiber to a control unit located outside the test area. The sphere consists of two hemispheres (complete with a center post much like an umbrella) which thread onto a plastic ring. A printed circuit board and battery packs are located inside the sphere. The center posts of each hemisphere contact the circuit board at the output of the RF link. The RF link consists of a laser modulated with the test signal, a length of optical fiber, an optical receiver in the sphere where the test signal is converted from optical back to electrical, an RF amplifier, a diode detector for amplitude control, a balanced-to-unbalanced transformer (balun), and a fixed load resistor to help match the amplifier to the sphere's impedance. The center posts tap the voltage seen across this load resistor and transfer it to the gap between the hemispheres. The diode detector, along with its circuitry and optical link to the control unit, is used to continuously monitor the RF drive voltage near the feed point on the amplifier side of the balun. This feature enables the operator to verify that the impressed voltage is the same from one test to another, and it also confirms that the unit is operating properly throughout a set of measurements.

A detailed description of the spherical radiator evaluation (angular patterns and intensity of the radiated fields) is given in Ref. [24] for the NIST prototype unit and in the next section for the unit used in this study. One aspect of these tests should be explained in the context of the construction and features of the radiator: the determination of the radiated field intensity. Although the voltage between the two center posts is continuously monitored, it does not enable us to directly calculate the radiated field. This is because the relationship between the voltage measured on the circuit board and the voltage realized at the equatorial gap in the spherical shell cannot be easily calculated or directly measured. Therefore the transfer function between the voltage we can measure on the circuit board and the radiated field was determined empirically. This was done by measurements on the NIST OATS and in the NIST anechoic chamber. The voltage between the center posts was fixed at some nominal value as indicated by the diode detector and voltmeter circuitry (usually 0.8 or 1.0 V) and the field intensity at the radiation pattern maximum was measured with a calibrated receiving system. The known radiation characteristics of a spherical dipole (see Ref. [24] for the formulation) were then used to calculate the realized voltage at the equatorial gap on the radiator. The free-space formula for the radiation pattern was used in the anechoic chamber, whereas on the OATS the ground plane reflections were taken into account. We can now compute the radiated field intensity or total power radiated into free space by using this measured transfer function to determine the realized voltage at the equatorial gap. This transfer function is called a scale factor in ref. [24], where values for the NIST unit may be found. The next section will detail this scale factor for the unit used in these tests.

Two other attributes of a characterized source are important for most applications and in particular for evaluating shielded room measurements. These are (1) repeatability and (2) loading effects caused by the measurement environment (shielded room). In other words, the source must not change over time, and the output must be insensitive to surrounding objects or conducting surfaces in order to have meaningful comparisons. The attributes of the spherical dipole were investigated recently and reported in Ref. [7]. We found that the spherical dipole source was repeatable within less than 0.55 dB at all but one measurement frequency and less than 0.1 dB at almost half the frequencies. The one point where it showed a difference of 0.93 dB was in the FM broadcast band, where there may have been some interference with the OATS measurement system. These differences are small compared to the variations noted for the shielded room environment and we feel comfortable that this source repeats well. The second attribute of the spherical dipole source examined in Ref. [7] was the question of loading, that is, the sensitivity of the source to nearby conducting objects. Some earlier results had indicated little or no loading effect in a mode-stirred chamber [24], at frequencies of 150 MHz and higher, for a dipole-to-wall separation of at least 1 m. At the lower frequencies (<50 MHz) in a small transverse electromagnetic (TEM) cell there appeared to be an effect on the order of 3 dB with the sphere 30 cm from the surrounding walls. A third set of measurements [7] was performed on the OATS facility at five selected frequencies with the sphere located from 0.25 to 2.25 m above the conducting ground plane. After correcting for the reflected signal at the receiving location, we determined that the radiated emissions were only slightly affected (~1 dB) by the ground plane except at the lowest test frequency (30 MHz) at a height of less than 0.5 m above the conducting surface. This effect was similar to that observed in the small TEM cell. We concluded from this evidence that any loading effects in the shielded rooms would be less than 1 or 2 dB, provided that the radiator is at least 0.5 m from conducting surfaces.

4. Calibration of the Standard Source

The spherical dipole radiator described in the previous section and in Refs. [6,7,24] was replaced with a commercial unit based on the NIST design for this series of experiments. This new unit contains essentially the same circuitry as the earlier NIST prototype but benefits from a redesigned circuit board and interior RF feed structure. This new radiator was carefully evaluated and calibrated in the NIST anechoic chamber and at the OATS before the shielded room measurements. These evaluation measurements include detailed radiation patterns (electric field) and gap voltage scale factor. The repeatability and stability of the unit can also be deduced because the measurements were repeated several times.

The radiated field measurements in the anechoic chamber were rendered at NIST. The radiator was mounted on a nonconductive tower attached to an antenna positioner near the center of the chamber. A calibrated receiving antenna was positioned 2 m from the radiator with the coaxial feedline extending away from the radiator and exiting the chamber. The polarization of the sphere and the receiving antenna were matched to provide maximum field coupling. The entire system, including the antenna positioner, was controlled by a computer in the adjoining equipment room. The software would adjust the amplitude of a signal generator driving the laser modulator to hold the detected voltage at the RF feed point in the sphere to a selected value and then read the signal on the calibrated receiving antenna. The sphere was rotated to a new position and the measurement process repeated for each data point.

This sequence gave us the radiated electric field patterns shown in figures 1, 2, and 3, which are representative of patterns throughout the spectrum from 30 to 1000 MHz. Three patterns are shown in each figure; one is calculated for an ideal spherical dipole [24] using an equivalent gap voltage excitation which produced the measured field maximum and the other two are measured data. The two measured patterns are similar (θ rotated 360°) but with the sphere positioned at $\phi = 0°$ and $\phi = 90°$. The ϕ reference on the sphere was the entry point for the optical fibers on the equator. The two patterns represent measurements where rotation in the θ direction brought the fibers either directly between the sphere and receiving antenna ($\phi = 0°$) or where the fibers were aligned along the axis of rotation ($\phi = 90°$). For convenience, the sphere was positioned in θ so that the dipole maximum or broadside radiation is at 0° and again at 180° as defined by the antenna rotator. Hence the rotation angle shown in figures 1 through 3 is related to θ by a 90° shift from the definition that $\theta = 0°$ is at the pole of the sphere (a null in the pattern) and the equator (gap) in the ϕ plane at $\theta = 90°$. The patterns shown in these figures and those measured at other frequencies indicate that the unit used in these tests maintained a good pattern throughout the frequency range of this study. The new circuit board and RF feed design have resulted in much improved radiation patterns at the higher frequencies over that reported in Ref. [24] for the NIST prototype.

The well-behaved radiation patterns indicated that the sphere was very close to ideal throughout the frequency range. This allowed us to predict the free-space radiated fields accurately using the formulas found in Ref. [24], provided that we had determined the gap voltage scale factor described in section 3 at each frequency. This scale factor amounts to adjusting the calculated radiated field pattern to match the measured field pattern. This is a simple process when the measured pattern is well-behaved as in this case. The indicated "gap voltage" at the output of the detector-voltmeter circuit is then scaled to provide the realized gap excitation voltage, which can then be used to calculate the radiated field in any direction from the sphere or to determine the total power radiated [24]. A graph of measured scale factors is given in figure 4 for the frequency range of 200 to 1000 MHz. The measurements were repeated several times and the results averaged; figure 5 is the standard deviation (sigma) of these data sets as a function of frequency.

5. Comparison Measurements Using the Standard Source

The concept of antenna factor is widely used in the EMI/EMC industry. The AF relates the incident electric field to the voltage at the terminals of the antenna measured by a receiver or spectrum analyzer. As a rule, the AFs are determined in an environment such as an OATS for a single geometry, and these factors are then used for a wide variety of measurements including those in shielded rooms. However, the actual AF is a function of the arrival angle and polarization of the incident wave, the proximity and orientation of reflecting surfaces, the proximity of other antennas including the equipment under test, etc. [25]. Also, small changes in the test geometry can result in a significant variation in the AF measured on an OATS [26, 27]. Since the OATS is often used as a reference facility for AF and emissions measurements, we performed some tests using the sphere to generate known fields for AF measurements.

The measurement data shown in figure 6 are four sets of AFs determined for a fixed length monopole receiving antenna placed directly on the NIST OATS. One set of data was measured with the NIST standard transmitting monopole as the transmitting antenna, at 12 m separation, to establish a known electric field and hence a 'true' AF. These measurements are estimated to be accurate within ±1.0 dB [28]. These results compare well with the second set of data, a numerical simulation using a version of the Numerical Electromagnetic Code (NEC). The last two sets of data were obtained with the spherical dipole as the transmitting source. The spherical radiator output had been previously calibrated using a horizontal receiving dipole to determine the gap voltage scale factor (see section 4). This factor and the equations for the transmitted field [24] were then used to predict the electric field incident upon the same monopole with the sphere in a vertical orientation 1 m above the ground plane and separated by either 3 or 4 m. In spite of all the changes to the measurement geometry and the various steps in the process, the sphere was able to generate the 'true' AFs of the fixed length monopole fairly well (largest deviation of about 2.5 dB). More work is needed before we can recommend that the spherical radiator become an alternative source for OATS AF measurements, but the technique is promising.

The shielded room environment will have significantly more influence on the AF of the receiving antenna than the OATS for the reasons we discussed in section 2. A determination of AF in a shielded room will necessarily include the net effect of the environment and the source on the antenna. As described in the following section, the receiving antenna's response was measured in three different shielded rooms using the spherical dipole as a standard source. The detected E field at each of the three participating laboratories were compared to the predicted E field on an OATS from the spherical dipole. The predicted E field is the theoretically calculated E field from the spherical dipole [24] corrected with the previously measured data from the NIST OATS measurements. The remaining reflections in the shielded rooms were intended to be included in the derived AF. The setup geometry in a shielded room was a separation distance of 1 m and a height of 1 m for both antennas, as specified in MILSTD 461/462. Figure 7 has the comparison of measured levels in each of the three laboratories to the predicted level for the vertically polarized E fields, and figure 8 has the comparison for the horizontally polarized E fields. Both figures show a nominal trend of comparison in the data with the expected variations in the shielded room data. These measured values were determined from AFs presently used at each laboratory.

A determination of the 'goodness' of this measurement data (figures 7, 8) can be obtained by looking at the distribution of the data about its average, that is, a histogram. This distribution is a count, at specified intervals, of the number of data points within an interval. For these data, the intervals studied are every 0.25 dB about the average. All of the frequency data are viewed together for simplicity. This histogram is shown in figure 9. The data show a maximum density at 0 dB, which is the average, and a standard deviation (95% confidence level) of ±3.6 dB. Also, 89% of the data are within ±5 dB of the average. This repeatability of the data is better than previously reported values [6,7]. Overall, the measurement of the spherical dipole at the three sites shows good correlation in the results obtained. However, the few outlying points from the average suggest a closer look at the measurement and its test environment.

6. Comparison Measurements of Shielded Rooms Using a Simulated EUT

The method that was used to reduce the variability in test data from shielded rooms was based on the spherical dipole source. This standard radiator compensated for the environmental effects of each individual room to provide better agreement in site-to-site results, and between OATS-to-shielded room results. The measurement plan was (1) to measure the emissions from a simulated equipment under test (S-EUT) at each site using a vendor calibrated antenna. Then, (2) to calibrate the receiving antenna in the shielded room environment using the spherical dipole source, and (3) to remeasure the emissions from the S-EUT using the sphere derived AFs (which now include the room effects for the present test setup). The final step is (4) to compare the measured emissions of the S-EUT using the vendor calibrated AFs to the measured emissions using the sphere derived AFs.

The S-EUT was a fixed length RF dipole antenna mounted on a tripod, figure 10, and provided with a constant amplitude, continuous wave (CW) signal. The CW RF signal source was a synthesized signal generator set at a constant amplitude and attached to a known length of coaxial cable. Vendor AFs are defined as the AF data provided with the antenna, and the sphere derived AFs are described later. Three laboratories, which perform MILSTD 461/462 RE102 tests on a regular basis, were chosen for this comparison. The intent here, as in the earlier test sequence [6,7], was to treat the S-EUT as a piece of electronic equipment sent to the laboratory for testing. We participated at each site with some of the measurements. We controlled the emissions from the S-EUT during the RE102 testing and also performed the in-room AF calibration of the receiving antenna using the spherical dipole source.

The frequency range of interest was 30 to 1000 MHz. This range is the calibrated range of the spherical dipole source. Frequencies of interest are every 10 MHz from 30 to 200 MHz, and every 50 MHz from 200 to 1000 MHz. The same setup geometry was maintained throughout the three laboratories. The S-EUT was placed at least 1 m above the room floor. The receiving antenna was 1 m from the S-EUT and its height was aligned with the center of the S-EUT. Both devices were at least 1 m from any walls, tables, etc., as prescribed by MILSTD 461/462 RE102.

6.1 Measurement Procedures for the S-EUT in a Shielded Room

A summary outline of the planned procedure:

(1) Calibrate all equipment as is normally done before a test.

(2) Place the S-EUT in location and a receiving antenna at a distance of 1 m from the S-EUT. Align the polarization of both antennas. Connect the S-EUT to the signal source with the calibrated cable, and the receiving antenna to the receiver with the test laboratory's cable(s). Seal the room.

(3) Since the output of the S-EUT is CW, set the first frequency and measure the emissions from the S-EUT using the receiver. Record these results, and proceed through the range of frequencies until all the frequency responses are recorded.

(4) Enter the shielded room and replace the S-EUT with the spherical dipole, the setup should be as in step 2, only the sphere is now in place of the S-EUT. Measure the response of the receiving antenna for a given output of the spherical dipole. This relation will determine a new set of AFs for this configuration. An automated sequence was used to set the sphere's output, via the gap voltage, and read a response from the receiving antenna to obtain the new set of AFs.

(5) Remove the sphere and place the S-EUT back in the same place as before (see step 2). The setup should be the same as it was originally. Repeat the measurement as described in step 3, only this time use the new AFs derived with the sphere to determine the emissions of the S-EUT.

Often, more than one antenna was needed to cover the required frequency range; then we repeated this procedure for each antenna until the data were measured for all frequencies. These data were taken with both transmitting and receiving antennas in the horizontal polarization and then both antennas in the vertical polarization.

We also wanted to check on the day-to-day variations of each site. Therefore, all measurements were repeated one additional time at each site. A repeat measurement involved resetting the antennas in the room and collecting another set of data on a different day.

The plan for the procedures assumed that each facility had identical equipment and test chambers. However, each site was slightly different in room layout and in test equipment, so the procedure was adjusted to accommodate each site.

The first site, which we will call Laboratory A, had a computer controlled system for the measurements. The room size was approximately 6.1 x 4.6 x 3.0 m (20 x 15 x 10 ft). Microwave absorber covered one wall and half of two other walls. We were able to perform the tests as planned. A biconical and a log spiral antenna were needed to cover the required frequency range. We did a measurement of the S-EUT using the vendor's AFs, then calibrated the receiving antenna with the sphere, and finally remeasured the S-EUT with the new sphere derived AFs. This gave us a set of data for each configuration that was tested at this facility. We did not get any horizontally polarized data at this site, only vertically polarized data.

At the second facility, Laboratory B, the measurements were performed once using their computer controlled system and the results calculated using a spreadsheet. Then, the receiving antenna's output was calibrated with the sphere, as described above, and the results recalculated using the new AFs and original readings of the S-EUT's output. The room size at this laboratory was 7.6 x 7.6 x 3.7 m (25 x 25 x 12 ft). The absorber material was on one wall and one half. A biconical and a log spiral antenna were also used here. Both horizontal and vertical polarizations were measured.

The third site, Laboratory C, had an automated system dedicated to perform the required MILSTD 461/462 RE102 tests and could not be easily reconfigured to perform our tests. Therefore, the measurements were recorded manually. The procedure was similar to the second site: only one measurement of the S-EUT, a calibration of the receiving antenna's output with the sphere, and two results (using the vendor AFs and the new sphere-derived AFs). A biconical and a ridged horn antenna were used here as the receiving antennas in both vertical and horizontal polarizations. The size of this room was 6.1 x 4.6 x 2.9 m (20 x 15 x 9.5 ft). The absorber material was on one wall and one half.

6.2 Comparison of Vendor AFs to Sphere-Derived AFs

The three participating laboratories will not be identified in this discussion of the results, and only their data will be considered.

Measurement of the AF for the receiving antenna were performed at each site as part of the test. These AFs were the ratio of the emitted E field of the spherical dipole source to the measured voltage of the receiving antenna in a shielded room. These AFs were measured for both horizontally and vertically polarized antennas. A summary of these measurements is shown in figure 11, along with the corresponding vendor AF data (solid line). Since each laboratory used its own antenna(s), results from each laboratory are shown separately. These data show there are differences of up to 20 dB between sphere or shielded room AF data and vendor AF data, depending on the frequency and laboratory. These differences are due, in part, to the room effects on the receiving antenna. This figure also shows the repeatability of each site for this measurement setup.

The average results, using vendor AFs, of the detected emissions of the S-EUT at all three sites are shown in figure 12. These results are for both vertically polarized and horizontally polarized E fields. The receiving antenna was polarization matched to the transmitting S-EUT. As figure 12 shows, the variation in the data from site to site is on the order of 25 dB with a few variations of 30 dB. This result is similar to the results from an earlier test done at the same laboratories [6,7]. The average results, using sphere derived AFs, of the detected emissions of the S-EUT at all three sites are shown in figure 13. These results show a clearer indication that one site is different than the other two. It appears to be a constant offset related to the receiving antenna. This figure (13) shows similar results as figure 12.

A comparison at each laboratory of the vendor AF results and the sphere derived AF results is given in figure 14. The difference in the detected E fields is determined by subtracting the detected E field using the sphere derived AFs from the field detected using the vendor AFs. This difference is directly related to the difference in AF at each laboratory. The difference in the detected E field, for each laboratory, is plotted in figure 15. This figure shows a maximum change in detected E field of 18 dB from vendor-derived to sphere-derived AFs. While most differences appear to be within ±5 dB, the larger differences could be at critical frequencies.

6.3 Repeatability and Site-to-Site Comparison

There are two types of variations to be studied, the day-to-day repeatability at each site and the site-to-site repeatability. For ascertaining the day-to-day variation at a particular laboratory, the difference between identical measurements taken on successive days is calculated for each frequency. This difference, called delta, is determined for both polarizations. The average, minimum, and maximum differences are then calculated using the difference data, in decibels, from all three sites. These results are plotted in figure 16 using the vendor AFs, and in figure 17 using the sphere-derived AFs. The dashed lines at ±5 dB are included to aid in facilitating discussion. For the vendor AF results; most of the data (82%) repeated within 5 dB, but at a few frequencies the site repeatability was as variant as 10 dB, and at two frequencies the day-to-day measurements reached a 15 dB difference. For the sphere-derived results, almost all (88%) of the day-to-day results repeated within 5 dB, and the extremes are less than those observed with the vendor AF results.

The question of site-to-site repeatability can be answered by viewing the S-EUT as an artifact that each laboratory measured and sent to the next laboratory. The results from each laboratory would be a single set of data versus frequency and an uncertainty associated with that data. The day-to-day repeatability is a good indicator of the uncertainty, so a single set of data must be derived for each laboratory. We calculated the average response at each site using the vertically polarized and horizontally polarized data (figures 12 and 13). One site (laboratory B) is offset from the other two laboratories over the entire frequency range. Also, the data from laboratory C appears to vary erratically above about 700 MHz; this could be due to equipment problems. The magnitudes of the average, minimum and maximum deviations from average are calculated from these average site responses. These deviations are plotted in figure 18 using all three sites and are also plotted using only laboratories A and C. The deviations are noticeably less when one is only viewing the two sites, A and C. Using only two sites, figure 19 compares the vendor results to the sphere results. The sphere derived data are closer to the average value and it's extremes are also less.

7. Conclusions

The results of the measurements are not as encouraging as originally hoped; however, there are some developments in the results that are worth mentioning. First, the day-to-day variations (figures 16 and 17) show that the repeatability at each site is on the order of ±5 dB. These data are independent of the receiving antenna's AF, and show the repeatability of each laboratory. This is fairly good for shielded room measurements. Next, the site-to-site variations (figures 18 and 19) show that the data obtained with the sphere-derived AFs are slightly more repeatable than the data obtained with the vendor AFs. The magnitude of this was not as large as we had expected; however, the improvement is real. Finally, the data obtained at laboratory B, even though it was repeatable with itself, showed a significant offset from the other laboratories. The reason for this offset is not obvious, but does suggest an attenuator or other calibration factor which was not accounted for in the data processing.

A final way to view the overall results from these data of the S-EUT is by looking at the distribution of the data about their average, that is, a histogram. This distribution is a count, at specified intervals, of the number of times a data point lies within an interval. For these data, the interval studied is every 0.25 dB about the average. All of the frequency data are viewed together for simplicity. This distribution, grouped every 5 dB, is shown in figure 20 for both the vendor AF and sphere-derived AF results. The resultant distribution with the sphere-derived AFs is more closely clustered about the average than the vendor AF distribution data. Almost 8% more of the data are within 5 dB of the average using the sphere-derived AFs, and within 10 dB there are 12% more data when using the sphere-derived AFs. Furthermore, none of the sphere-derived AF data are more than 20 dB from the average. This definitely is an improvement in repeatability, even though it is a small one.

Even though the sphere-derived AF data show slight improvement in repeatability over the vendor AF data, it may not be practical to expect significant improvements at all frequencies for routine MILSTD 461/462 tests on more complicated sources. The data collected during these tests indicate that other factors in the shielded room environment (discussed in section 2) have such a detrimental effect on repeatability as to mask the benefits of using more accurate antenna factors. A more sophisticated calibration technique may be necessary to include these highly variant effects into the derivation of antenna factor.

However, laboratories performing MILSTD 461/462 tests should strive to reduce the large day-to-day variations by careful controls over the measurement layout in the shielded room, increased use of absorbing materials, and recognizing special conditions such as room resonances. Also, a program using a simulated EUT source as a laboratory intercomparison may help to reduce the variability in the data from site to site. These actions, along with incorporating the in-situ AF measured with a standard source, should help achieve better agreement between measurements performed at any laboratory using a shielded room environment.

We thank the Naval Air Systems Command (NAVAIR) for their funding and support of this project. We also thank the three laboratories for their participation in this project, especially the individuals who helped perform the measurements. And finally, we thank the Electromagnetic Interference Laboratory of the Naval Air Warfare Center at Pax River, MD, for their unbridled support of this project.

8. References

[1] Krstansky, J.; Standley, R. Theory of RFI measurements in shielded enclosures. 8th Ann. IEEE Natl. Symp. on Electromagnetic Compatibility, San Francisco, CA; July 1966.

[2] Free W.R. Radiated EMI measurements in shielded enclosures. 1967 IEEE Electromagnetic Compatibility Symp. Record, Washington, DC; July 1967.

[3] Stuckley C.; Free W.R.; Robertson D. Preliminary interpretation of near-field effects on measurement accuracy in shielded enclosures. 1969 IEEE Electromagnetic Compatibility Symp. Record, pp. 119-127; Asbury Park, NJ; 17-19 June 1969.

[4] Donaldson, E.E.; Free, W.R.; Robertson, D.W.; Woody, J.A. Field measurements made in an enclosure. Proc. IEEE, Vol. 66, No. 4; April 1978.

[5] Cruz, J.E.; Larsen, E.B. Assessment of error bounds for some typical MIL-STD-461/462 types of measurements. Nat. Bur. Stand. (U.S.) Tech. Note 1300; 1986 October. 108 p.

[6] Koepke, G.; Randa, J. Results of screened-room measurements on NIST standard radiators. Natl. Inst. Stand. Technol. NISTIR 5010; 1993 October. 34 p.

[7] Koepke, G.; Randa, J. Screened-Room Measurements on the NIST spherical-dipole standard radiator. J. Res. Natl. Inst. Stand. Technol. 99(6): 737-749; 1994 Nov.-Dec.

[8] Military Standard (1993). Requirements for the control of electromagnetic interference emissions and susceptibility. MIL-STD-461D (companion document to MIL-STD-462D).

[9] Military Standard (1993). Measurement of electromagnetic interference characteristics. MIL-STD-462D (companion document to MIL-STD-461D).

[10] Van Steenberg, G.N.; Dolle, W.C.; Willman, J.F. Shielded enclosure measurements can be accurate. 21st An. Southwestern IEEE Conf. and Exhibition, San Antonio, TX; 1969 April 23-25.

[11] Cruz, J.E.; Larsen, E.B. Alternative techniques for some typical MIL-STD-461/462 types

of measurements. Natl. Inst. Stand. Technol. Tech. Note 1320; 1989 March. 44 p.

[12] Marvin, A.C.; Steele, L. Improved techniques for the measurement of radiated emissions inside a screened room. Electron. Lett. Vol. 22(2): 94-96; 1986 January 16.

[13] Steele, L.; Marvin, A.C. New screened room techniques for the measurement of RFI. 5th Int. Conf. on Electromagnetic Compatibility, Pub. No. 71; York, UK; 1986.

[14] Herring, J.L.; Duffy, A.P.; Benson, T.M.; Christopoulos, C. A transmission-line modeling (TLM) study of screened room behavior, IEE Colloquium on Radiated Emission Test Facilities; Dig. no. 132; IEE, London, UK; 1992 June 2.

[15] Duffy, A.P.; Naylor, P.; Benson T.M.; Christopoulos, C. Coupling measurements and comparisons with simulations inside a screened room. 8th Int. Conf. on Electromagnetic Compatibility; Pub. no. 362; pp. 108-114; IEE, London, UK; 1992 September 21-24.

[16] Goodwin, S.; Marvin, A.C. An analysis of the effects of cable layout on cable to antenna coupling inside a screened room. IEEE Trans. Electromagnetic Compatibility; 33(3); 163-171; 1991 August.

[17] Bates, T. Reduction of em wave reflections in a shielded room. IEE Colloquium on EMC and the Motor Vehicle; Dig. no. 168; IEE, London, UK; 1990 November 29.

[18] Cook, R.J.; Bansal, P.S.; Alexander, M.J. The measurement of field strength in a screened enclosure. 8th Int. Conf. on Electromagnetic Computability, Pub. no. 362; IEE, London, UK; 1992 September 21-24.

[19] Marvin, A.C.; Goodwin, S. Field coupling to antennas in screened enclosures. IEE Colloquium on Calibration of Antennas for Close Range Measurements; Dig. no. 18; IEE, London, UK; 1990 January 24.

[20] Marvin, A.C.; Mann, S.M. Experimental study of the calibration of antenna-screened enclosure combinations for radiated emission measurements in the frequency range from 1 to 30 MHz. IEE Proc. Sci., Meas. Technol.; 141(4); 278-282; 1994 July.

[21] Marvin, A.C.; Dawson, L. New developments in the calibration of screened enclosure-antenna combination for radiated emission measurements in the 1 MHz to 30 MHz frequency range. 9th Int. Conf. on Electromagnetic Compatibility; Pub. no. 396; IEE, London UK; pp. 28-33; 1994 September 5-7.

[22] Society of Automotive Engineers. EMI measurement antennas, standard calibration method. SAE ARP 958, Rev. A; Society of Automotive Engineers; Warrendale, PA, 1992.

[23] Crawford, M.L.; Workman, J.L. Spherical dipole for radiating standard fields. Proc. CPEM; 1980 June 23-27.

[24] Koepke, G.; Driver, L.; Cavcey, K.; Masterson, K.; Johnk R.; Kanda, M. Standard spherical dipole source. Natl. Inst. Stand. Technol. Tech. Note 1351; 1991 December.

[26] Bennett, W.S. Antenna factors in EMC measurements. IEEE 1983 Int. Symp. on Electromagnetic Compatibility, Arlington, VA; pp. 34-37; 1983 August 23-25.

[27] Millen, E.M.; Friesen, D.R. Test geometry influence on antennas used for MIL-STD-461/462 testing. IEE Colloquium on Calibration of Antennas for Close Range Measurements; Dig. no. 18; IEE, London, UK; pp. 4/1-3; 1990 January 24.

[28] Camell, D.G.; Larsen, E.B.; Cruz J.E.; Hill, D.A. NIST calibration procedure for vertically polarized monopole antennas, 30 kHz to 300 MHz. Natl. Inst. Stand. Technol. Tech. Note 1347; 1991 January. 28 p.

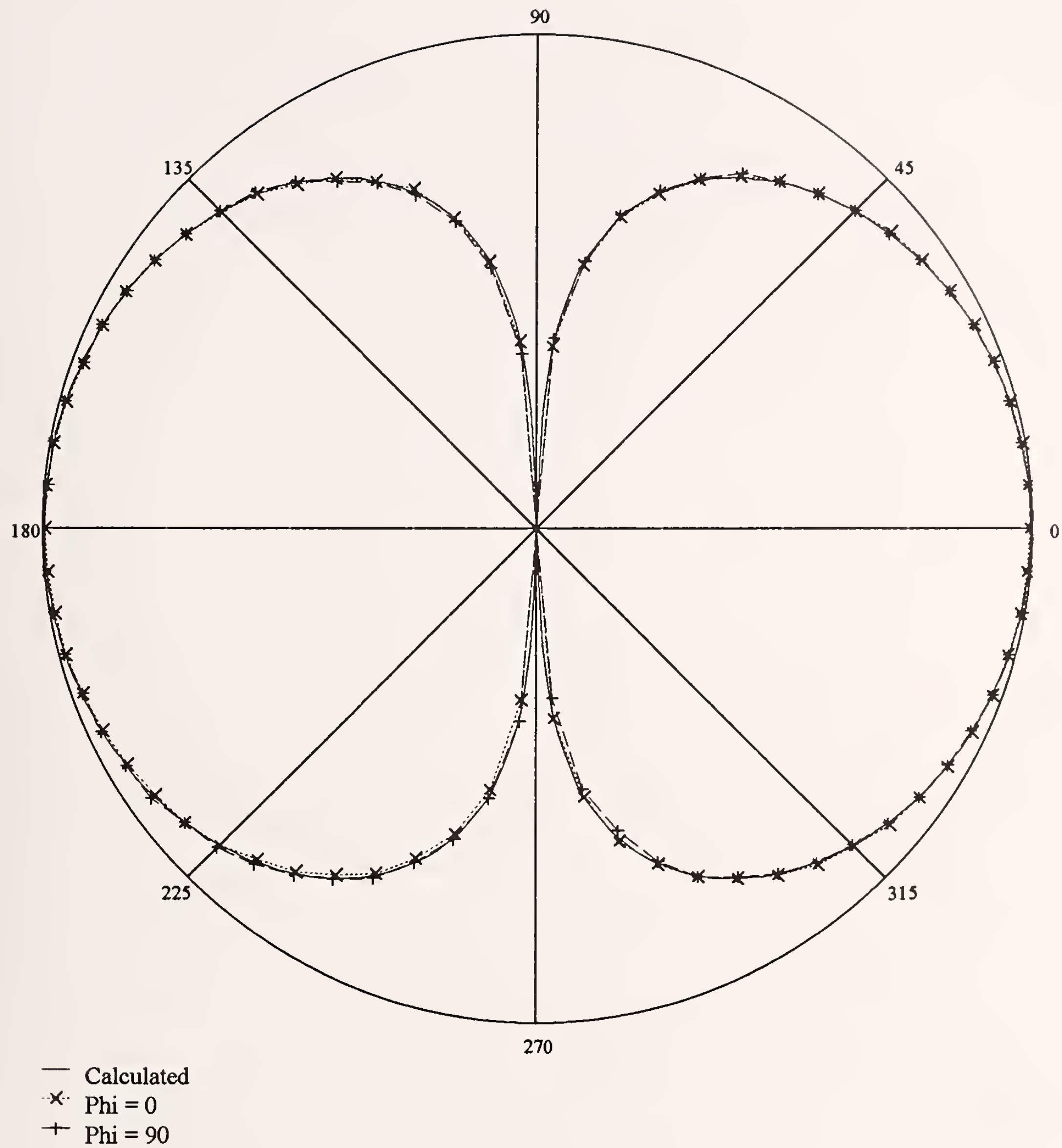

Figure 1. Radiated E-field patterns of the spherical dipole radiator at 200 MHz.

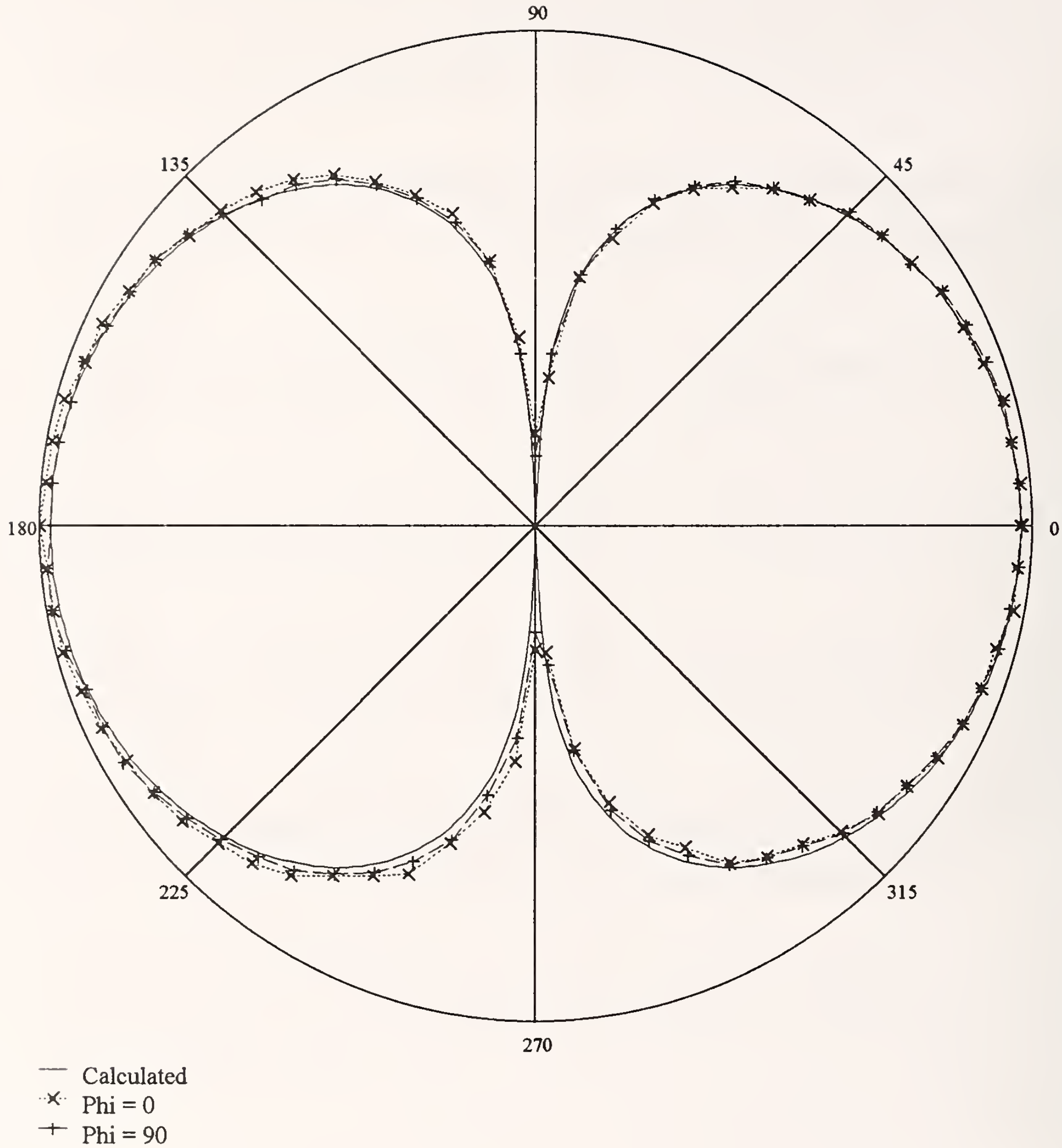

Figure 2. Radiated E-field patterns of the spherical dipole radiator at 600 MHz.

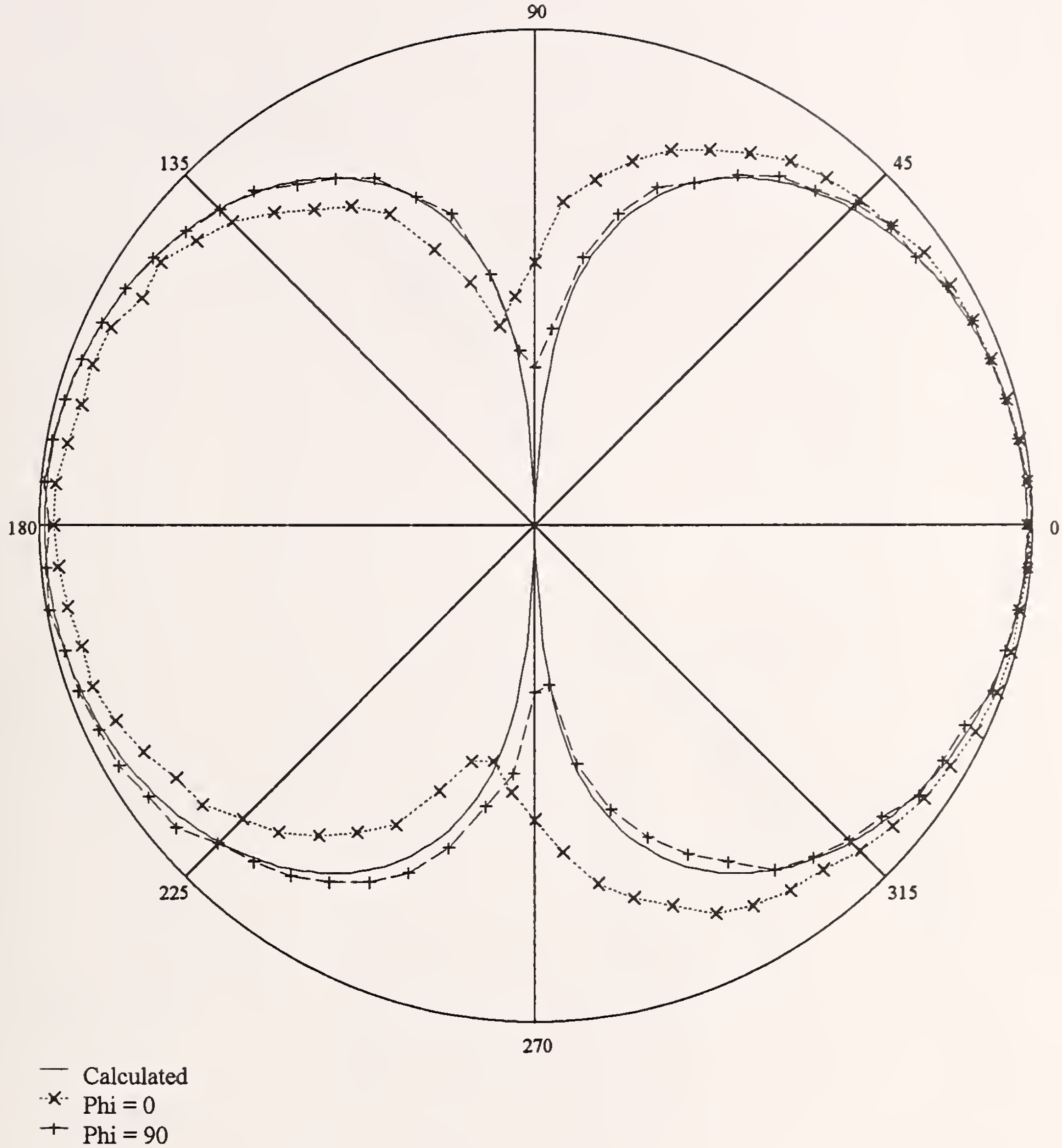

Figure 3. Radiated E-field patterns of the spherical dipole radiator at 1000 MHz.

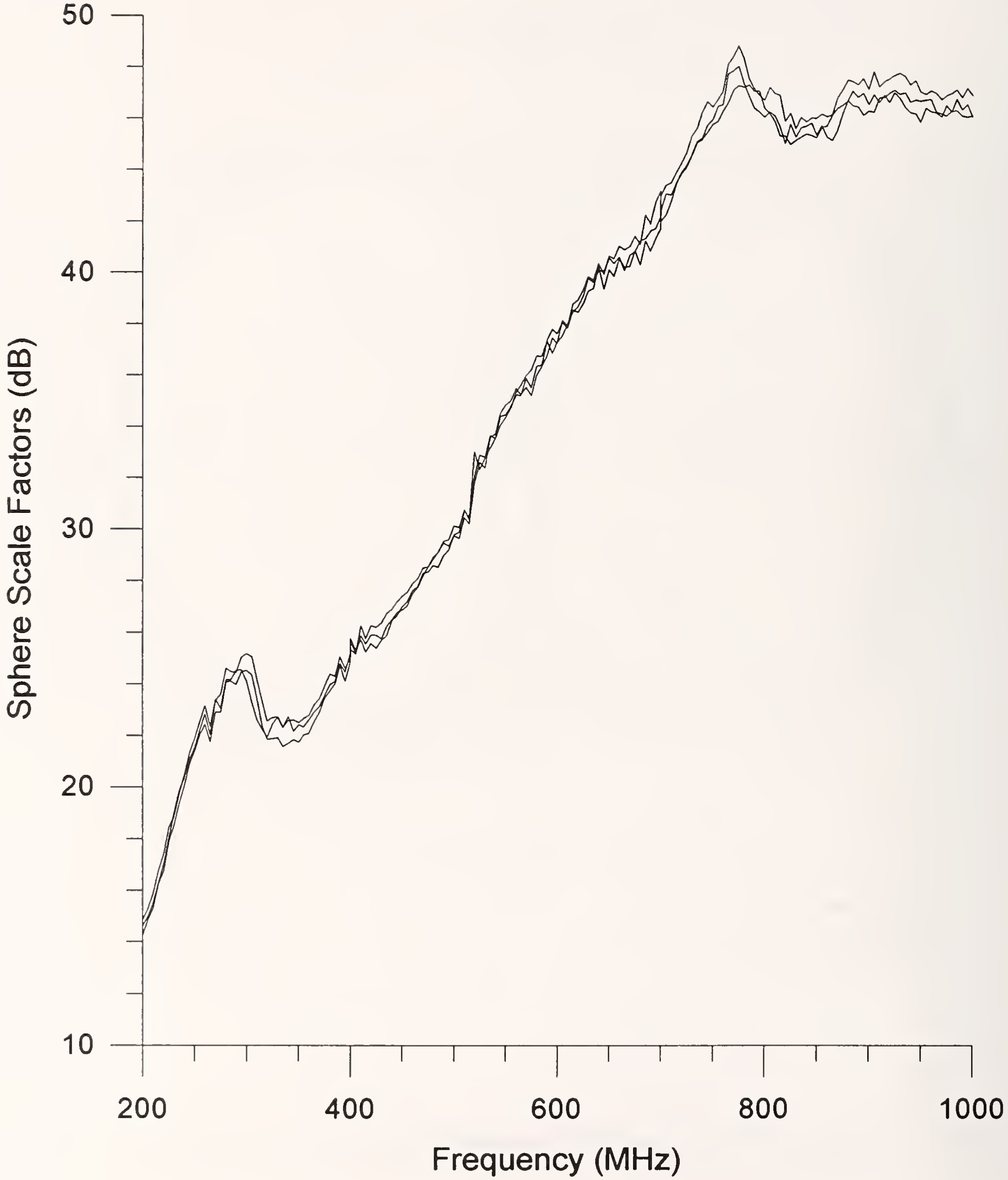

Figure 4. Measured scale factor of the spherical dipole radiator from 200 to 1000 MHz.

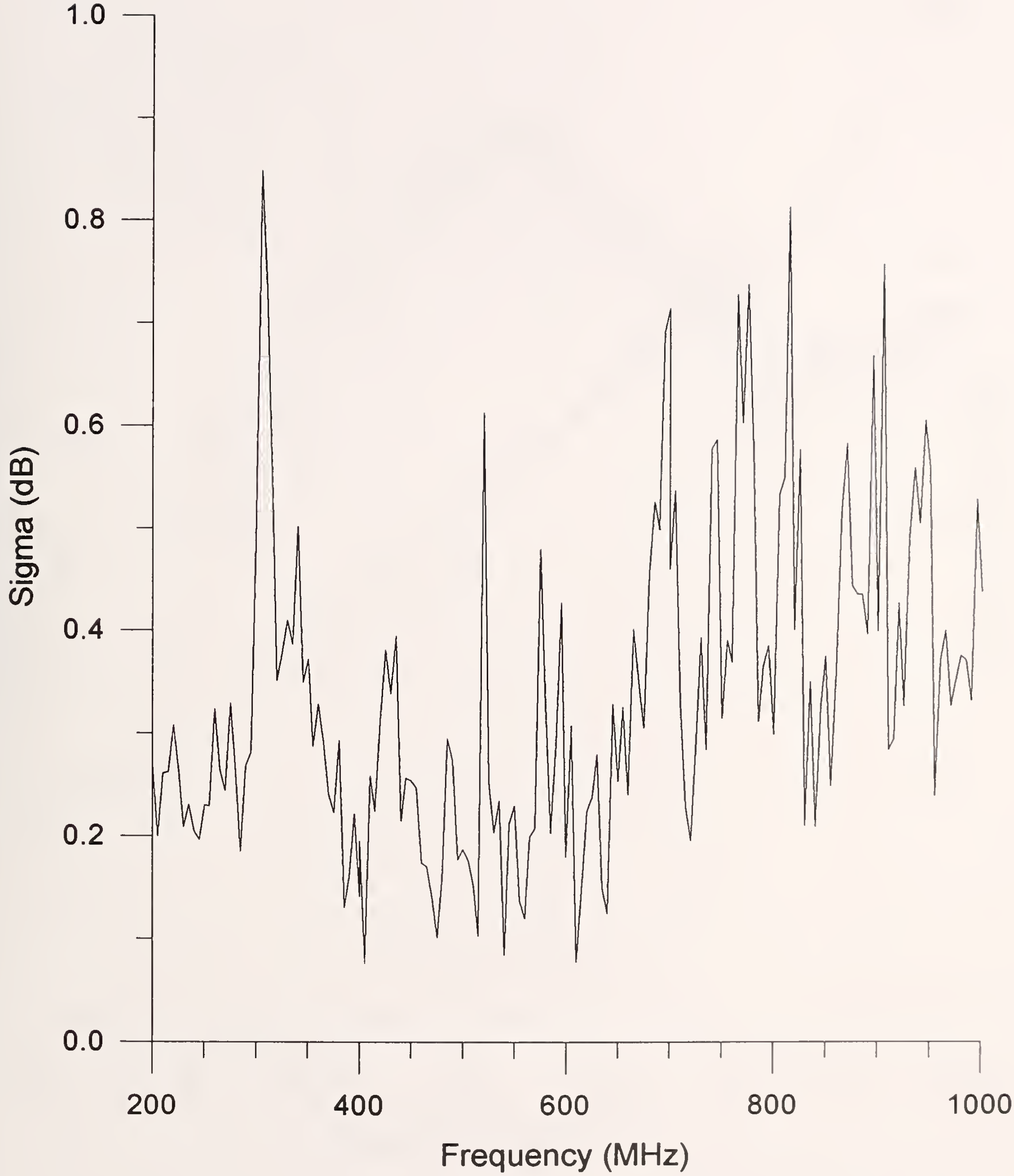

Figure 5. Standard deviation of the scale factor data for the spherical dipole.

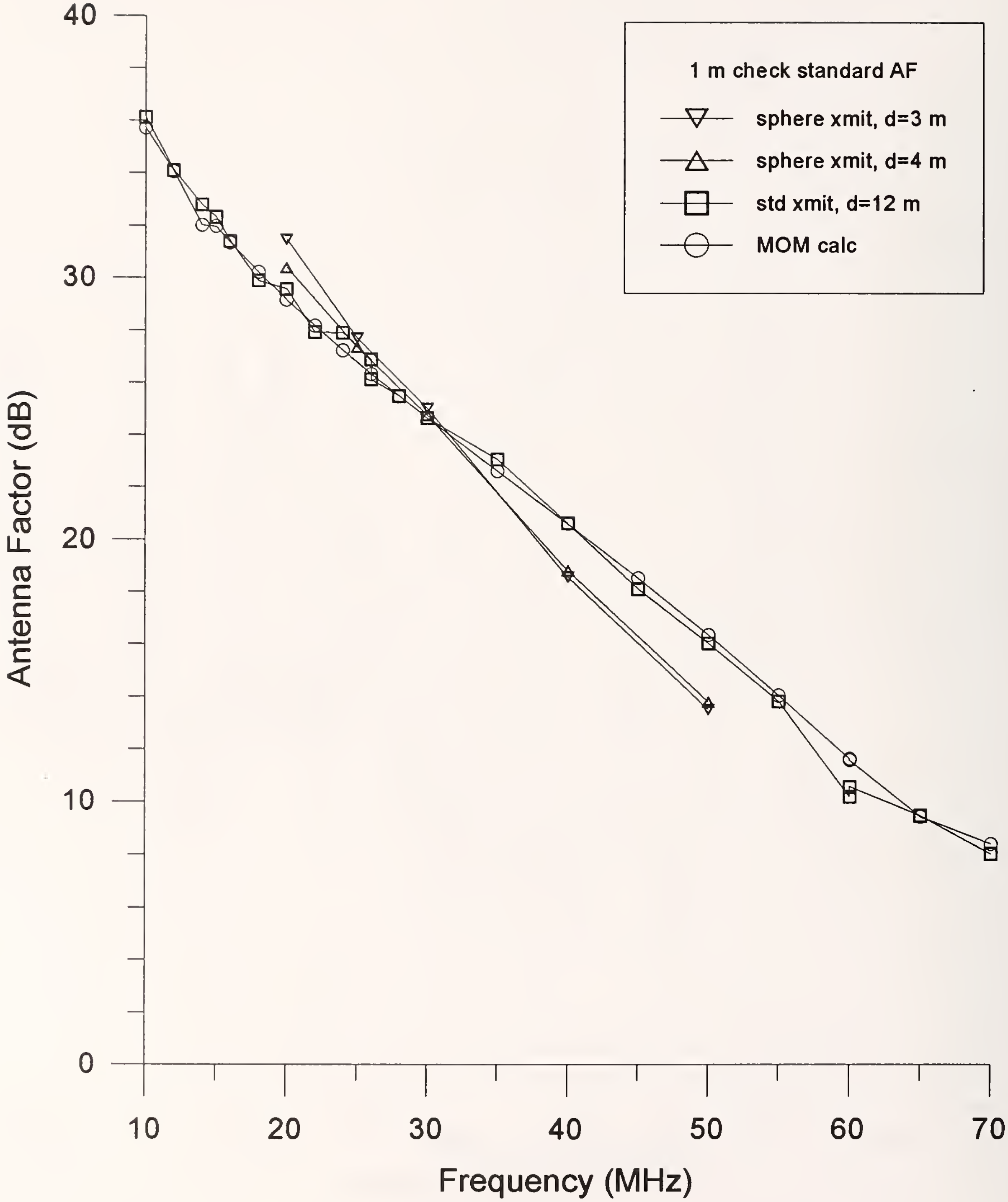

Figure 6. Comparison of measured and calculated antenna factor for a 1 m passive monopole.

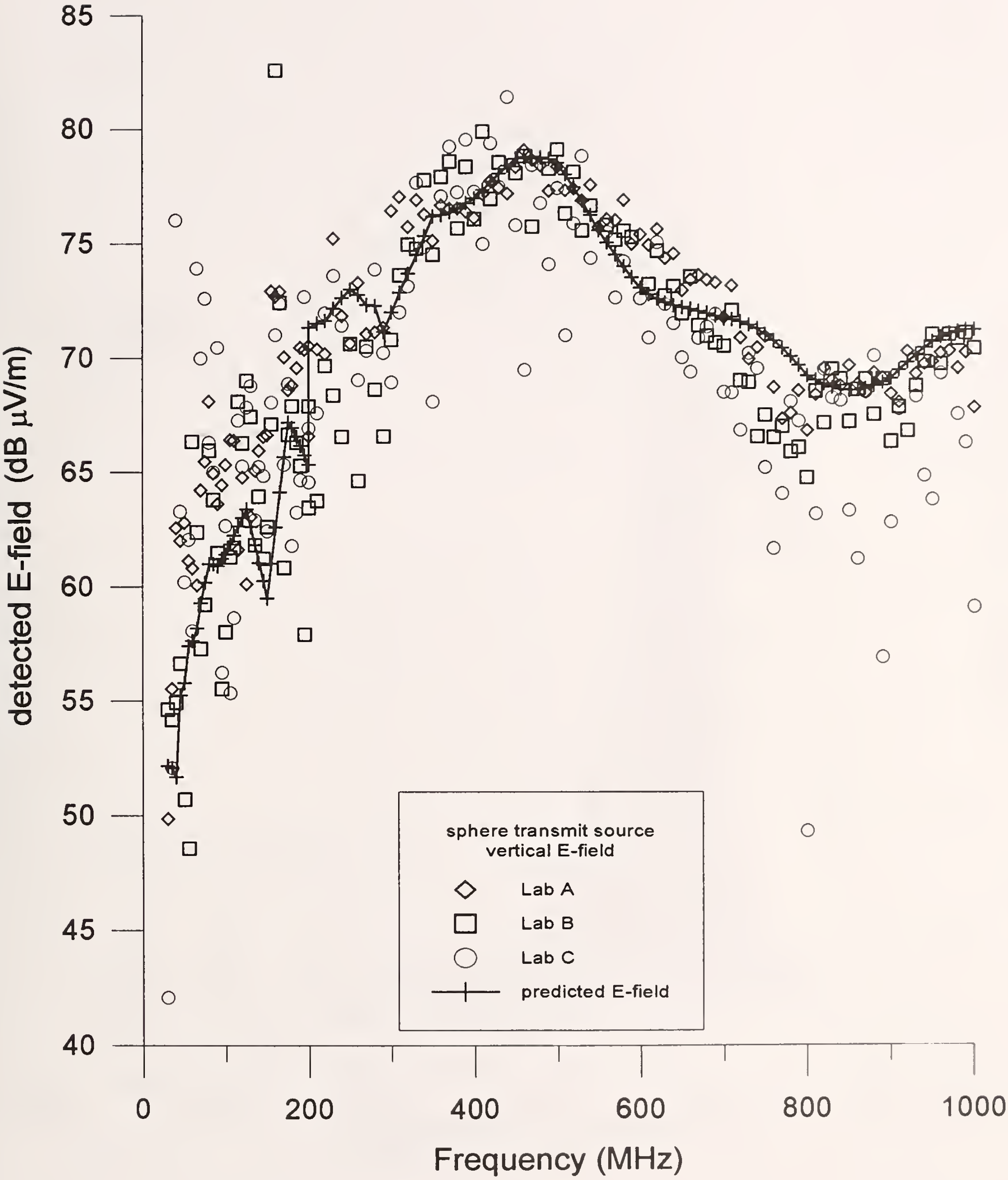

Figure 7. Comparison of predicted and detected vertically polarized emissions of the spherical dipole in three shielded rooms.

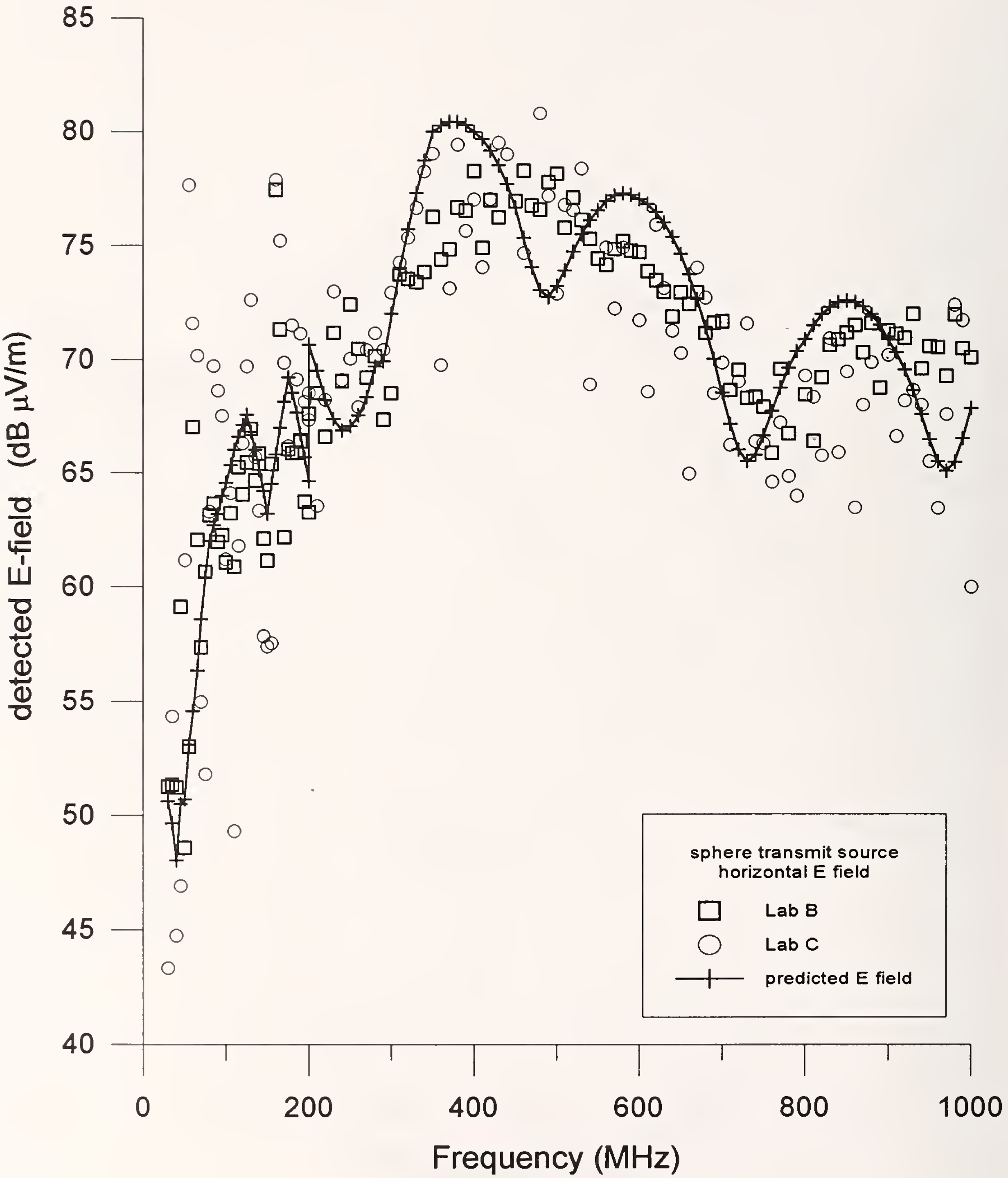

Figure 8. Comparison of predicted and detected horizontally polarized emissions of the spherical dipole in two different shielded rooms.

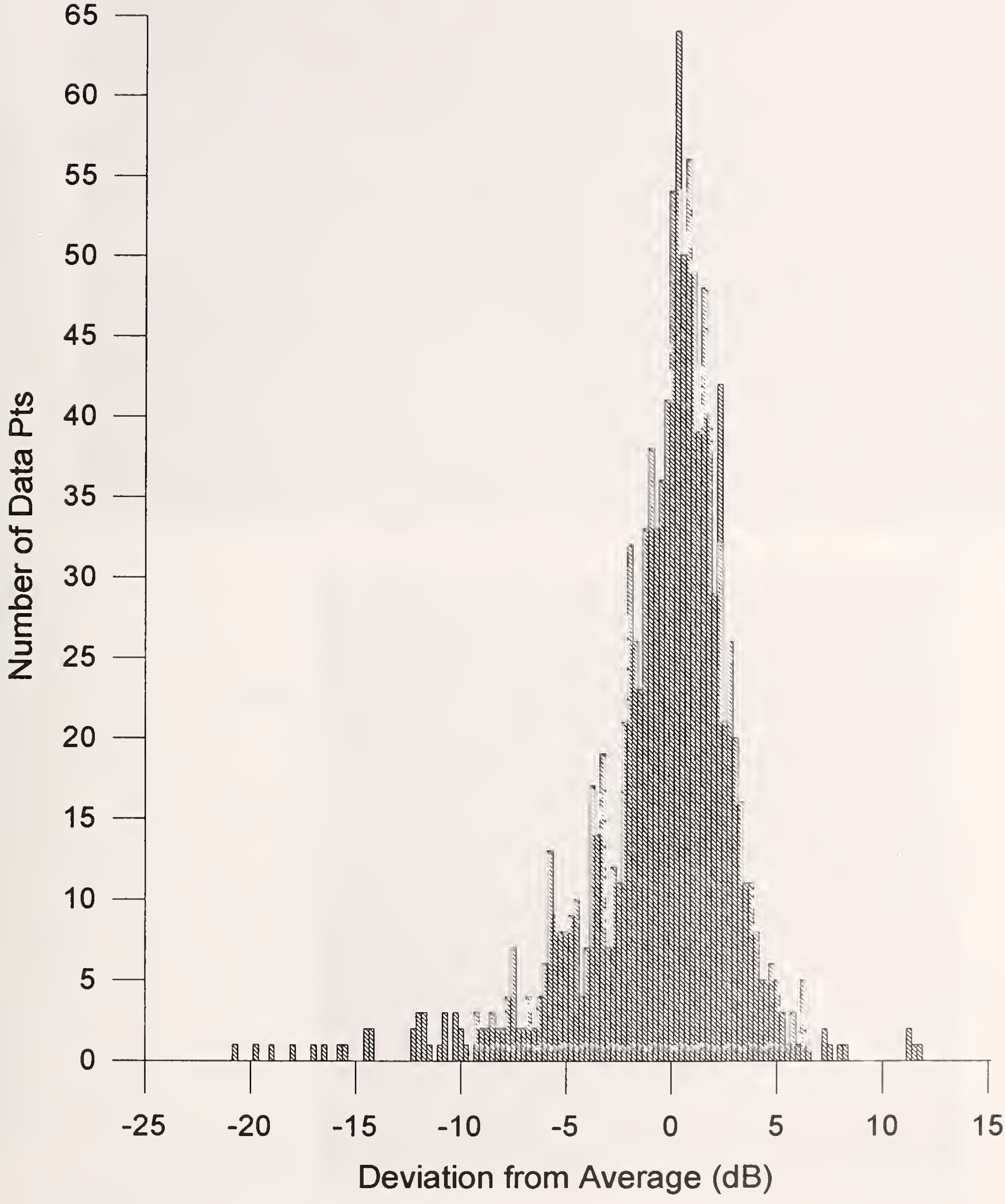

Figure 9. Distribution of data about the average on measured emissions from the spherical dipole in three different shielded rooms.

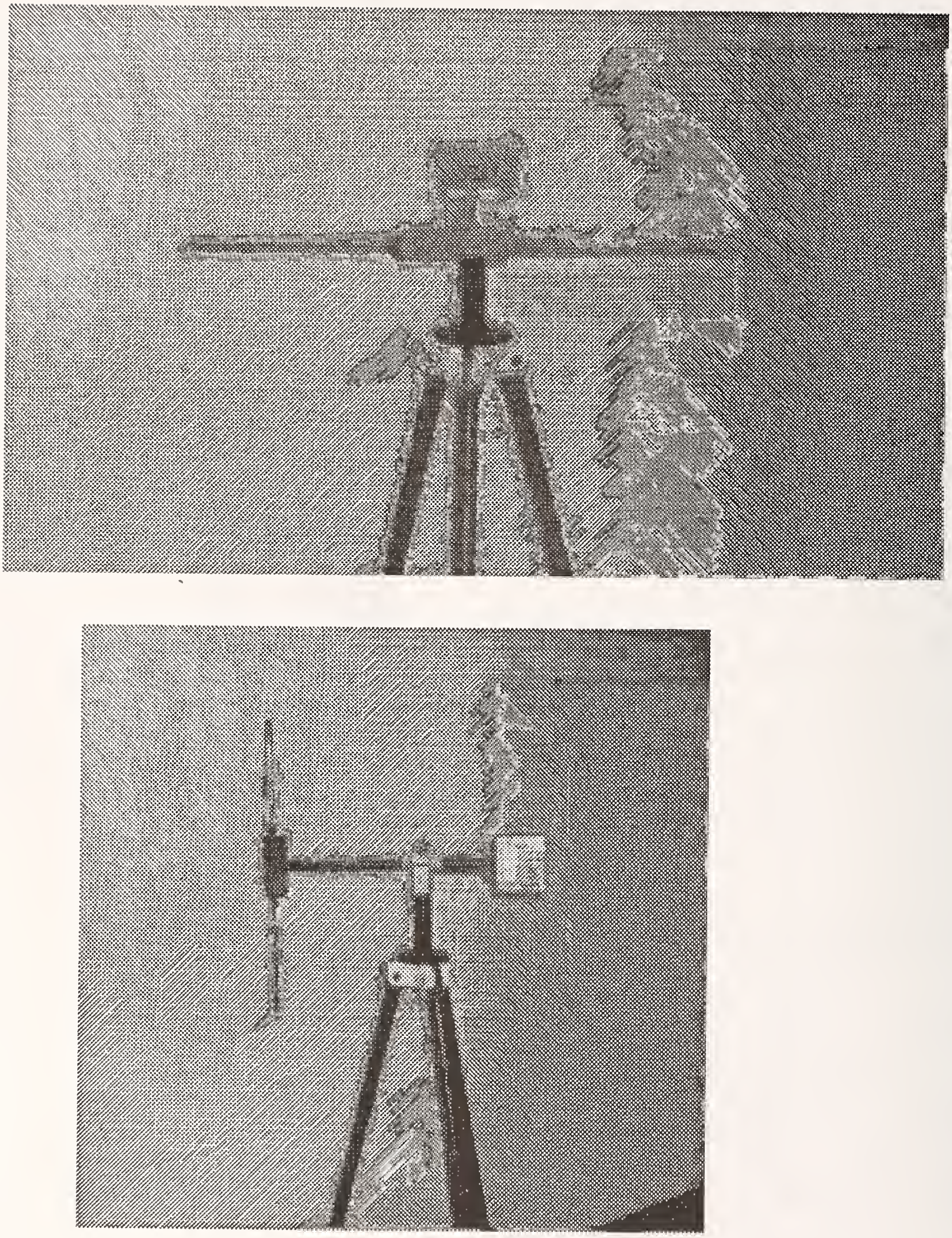

Figure 10. Photos of the simulated EUT (S-EUT) used at three shielded room laboratories.

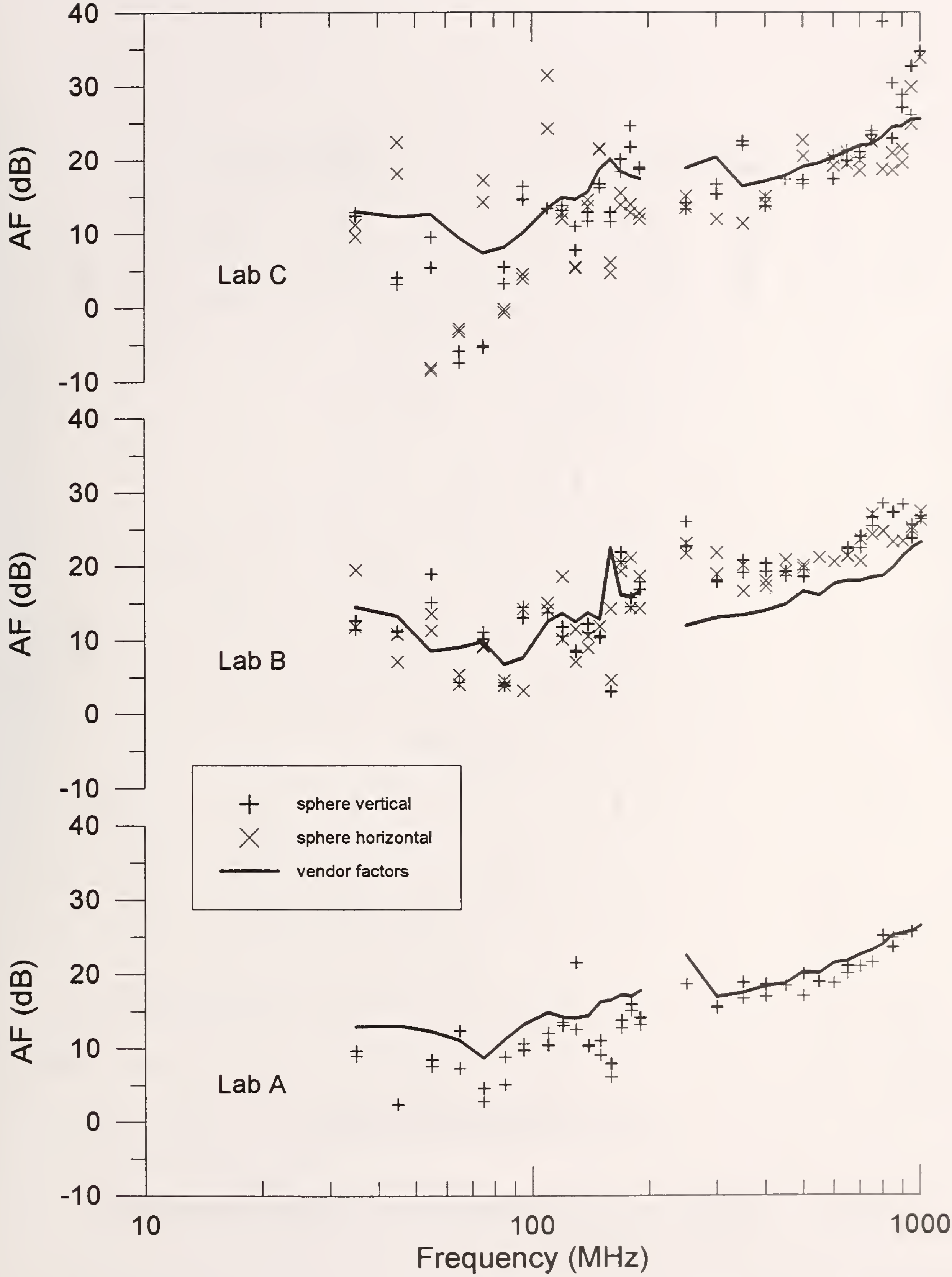

Figure 11. Comparison of vendor and sphere-derived antenna factors at each site.

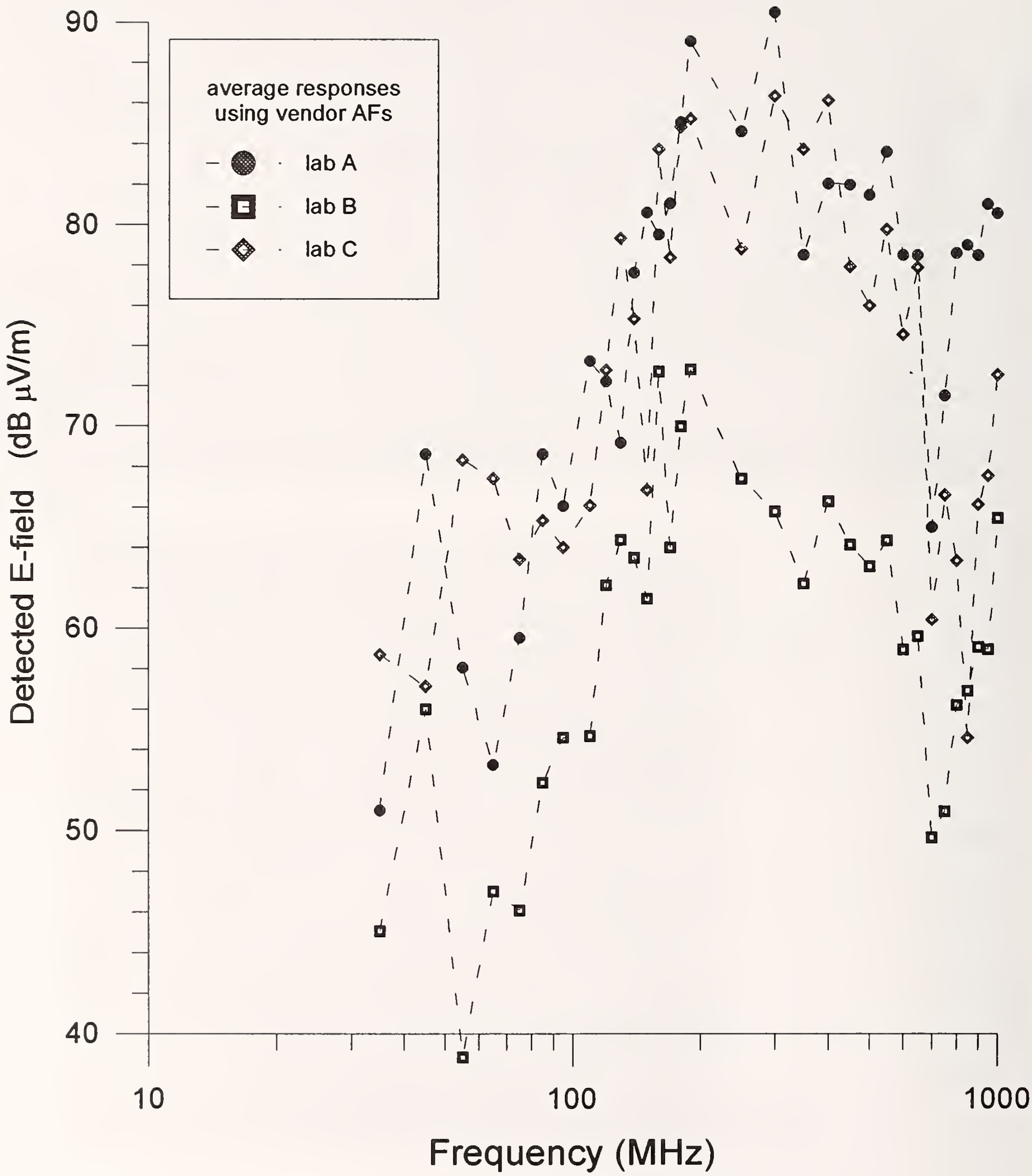

Figure 12. Average detected emissions from the S-EUT for three laboratories using the vendor AFs.

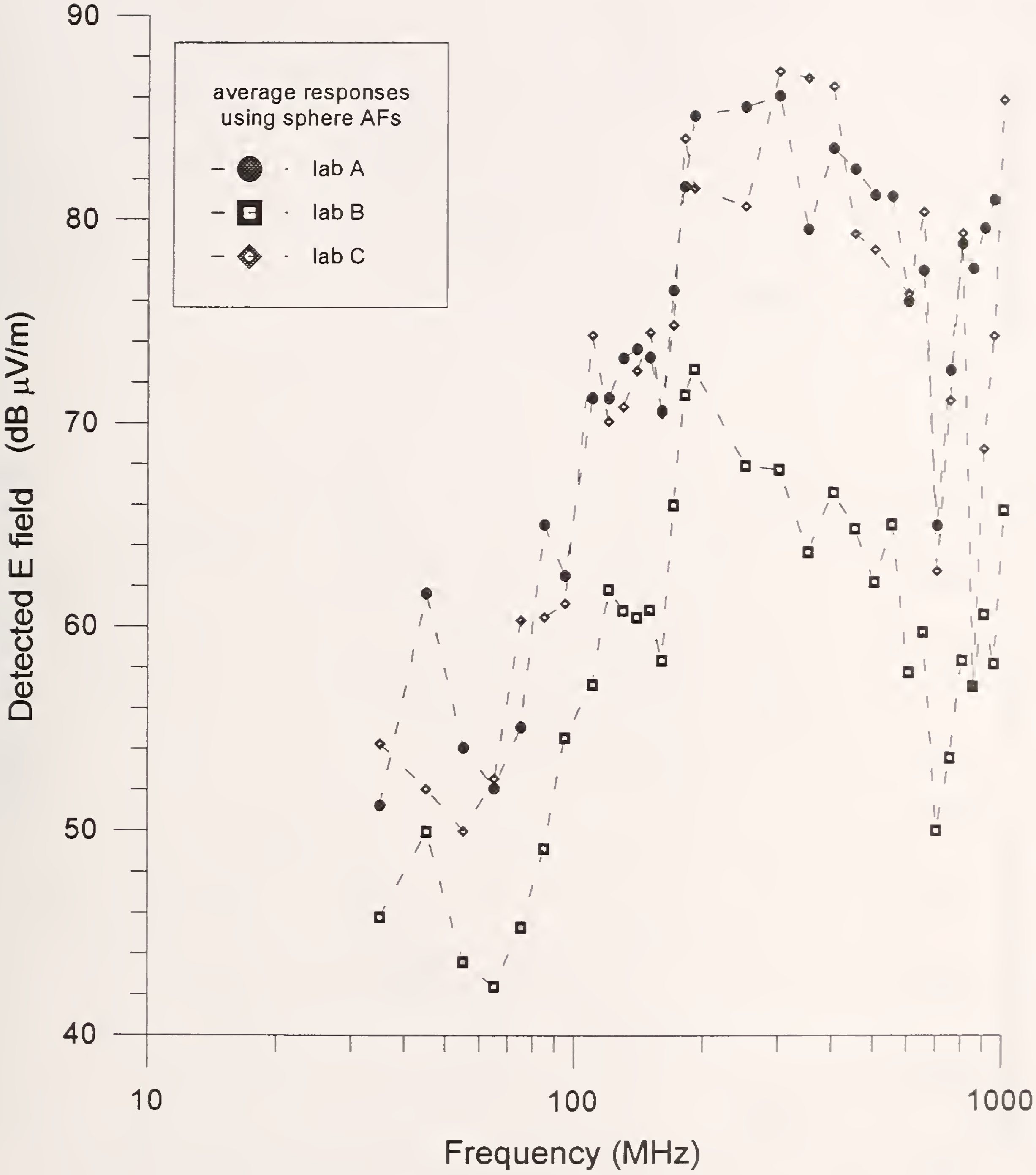

Figure 13. Average detected emissions from the S-EUT for all three laboratories using the sphere-derived AFs.

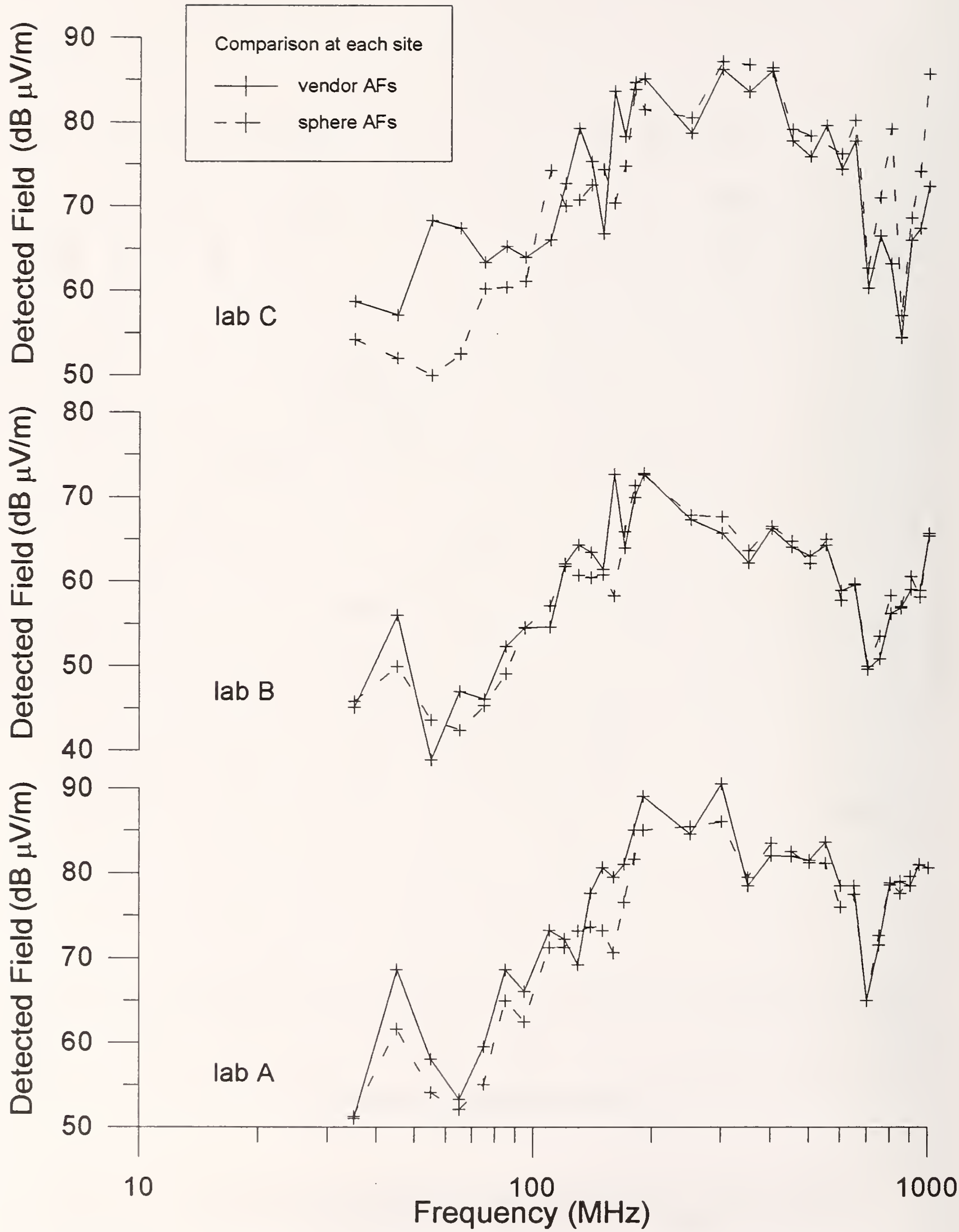

Figure 14. Comparison of detected emissions from the S-EUT at each of the three laboratories using both vendor and sphere-derived AFs.

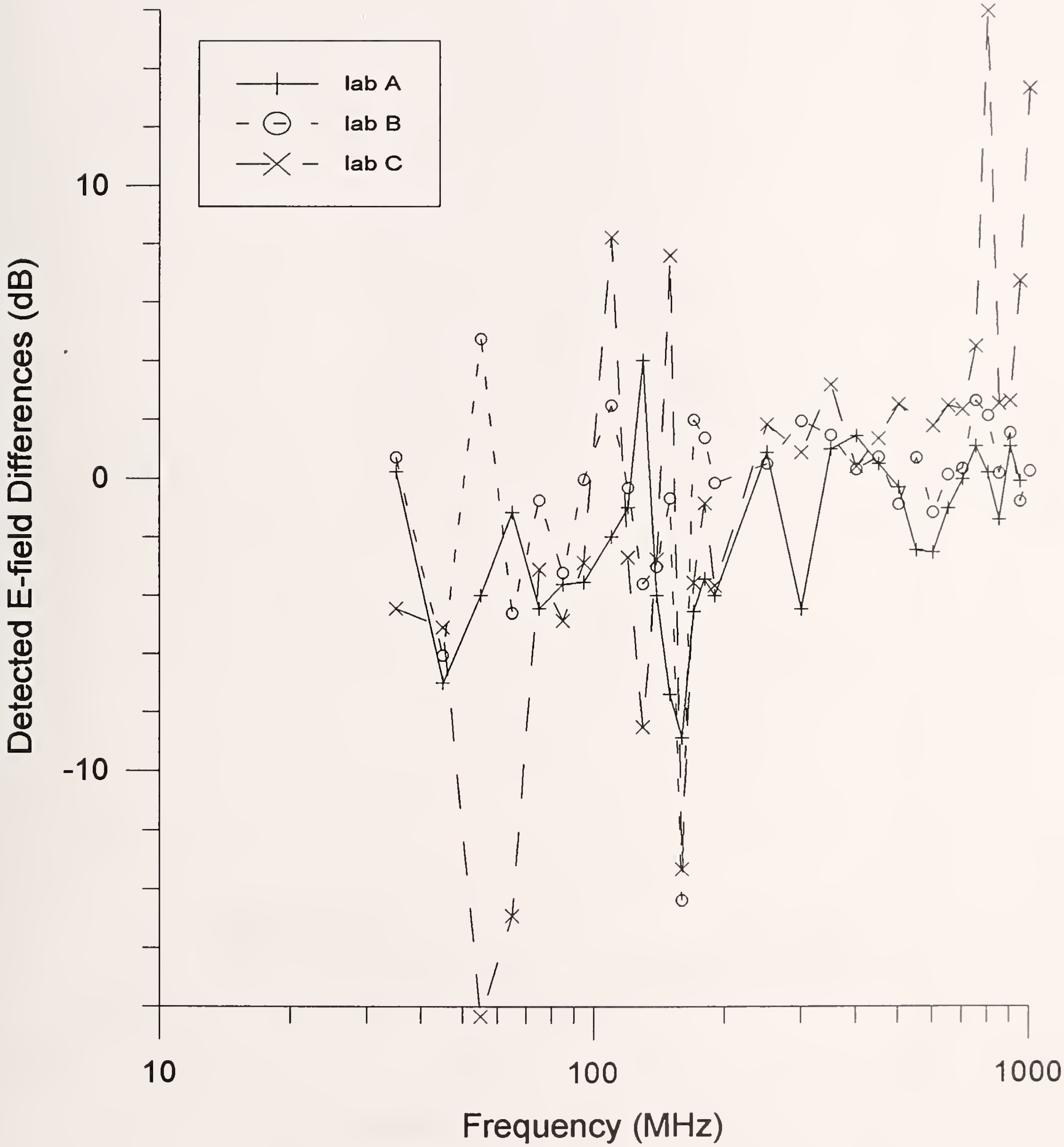

Figure 15. Differences in the detected emissions from the S-EUT between vendor and sphere-derived AF data.

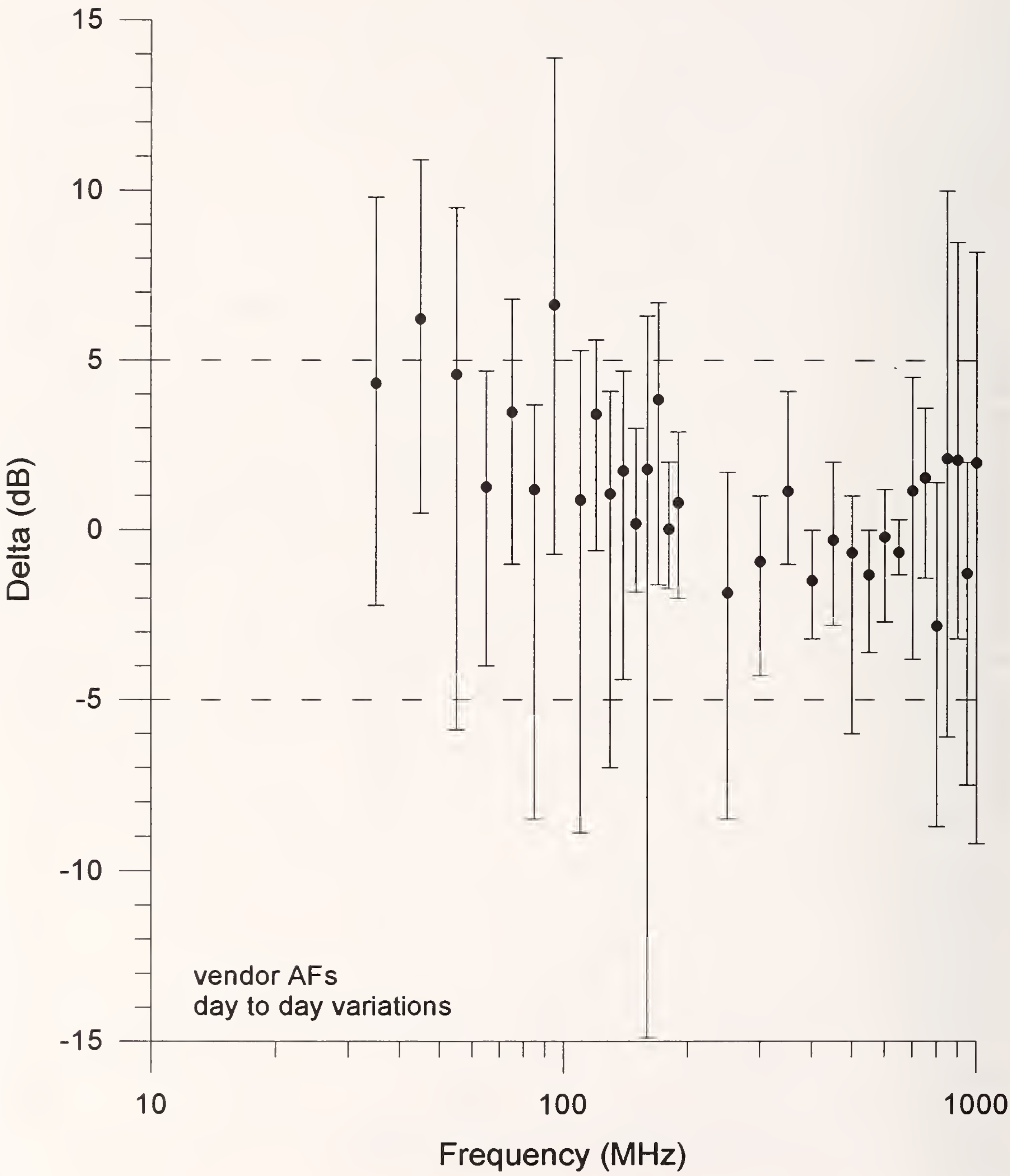

Figure 16. Day-to-day variations of the detected emissions of the S-EUT from all three laboratories using the vendor AFs.

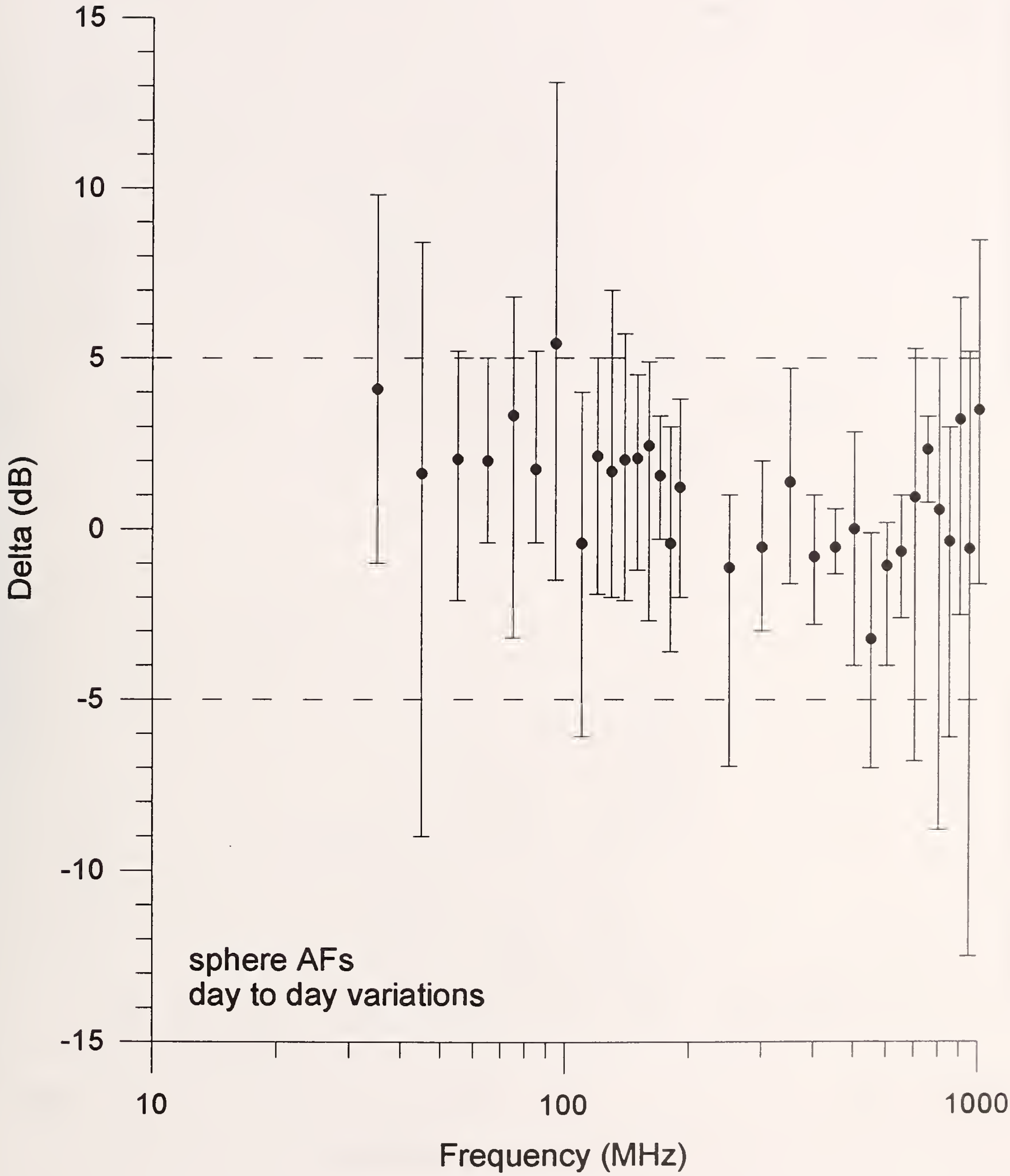

Figure 17. Day-to-day variations of the detected emissions of the S-EUT from all three laboratories using the sphere-derived AFs.

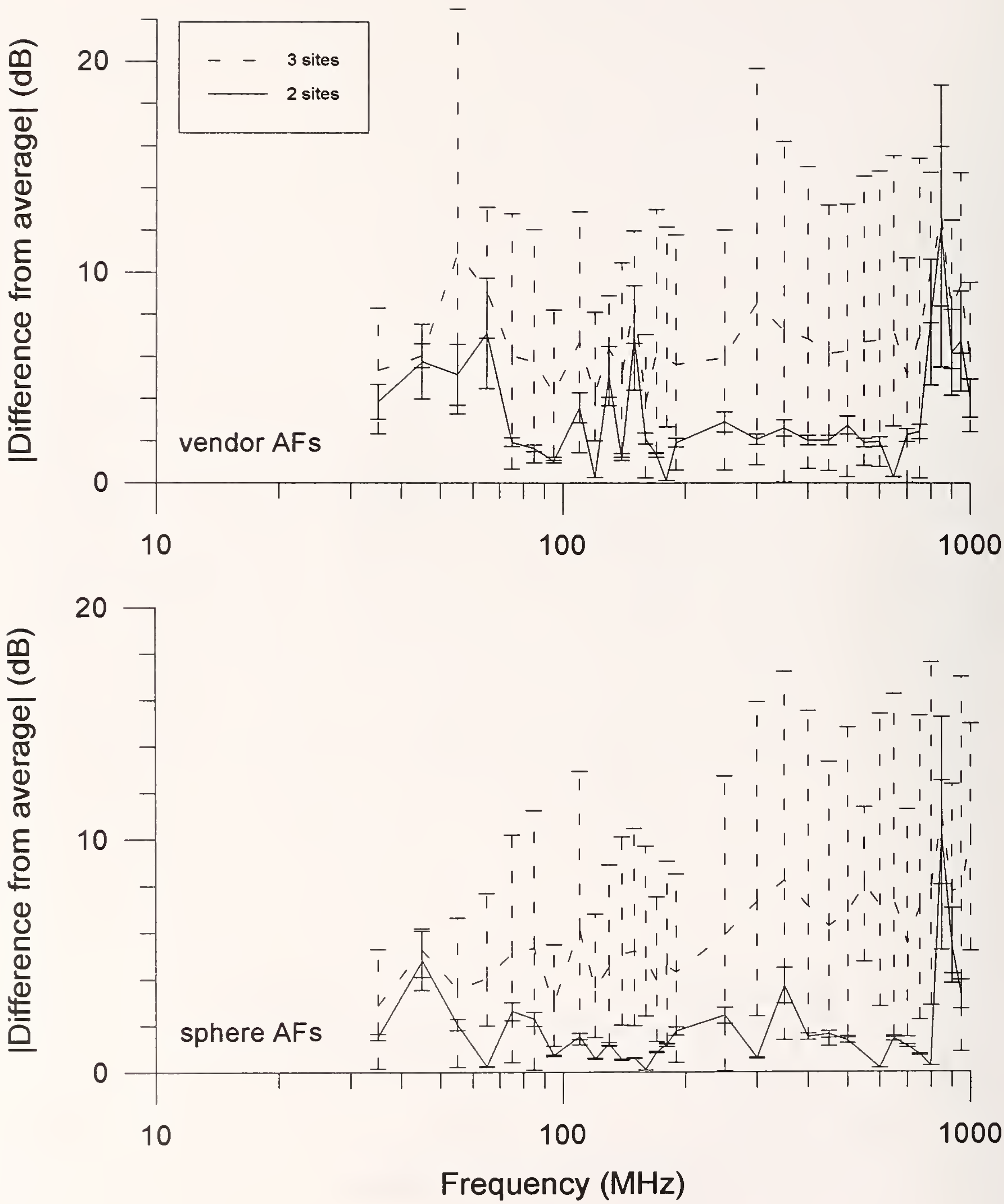

Figure 18. Comparison of variations in detected emissions from the S-EUT using three-site data and two-site data, for both vendor and sphere-derived AFs.

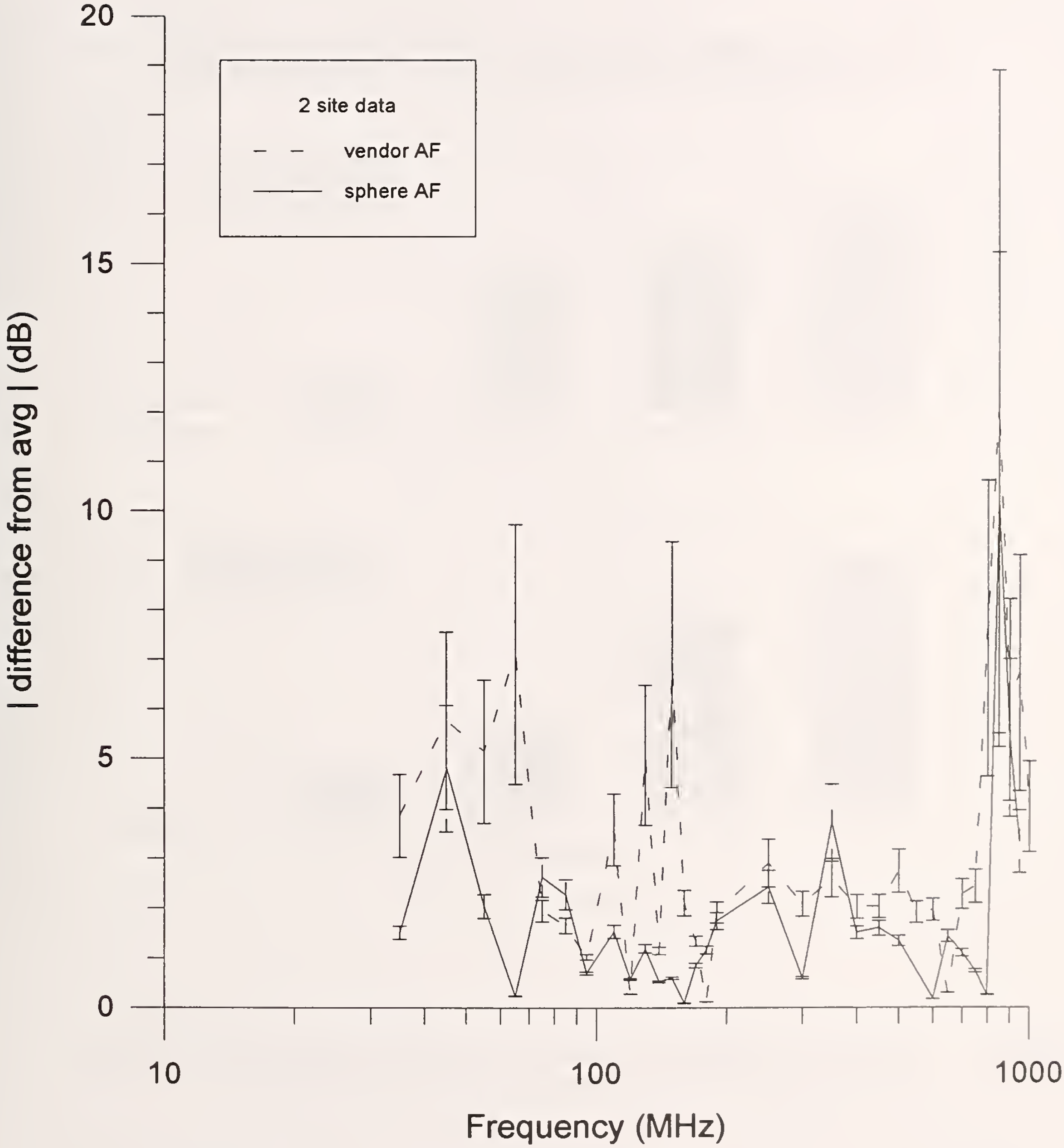

Figure 19. Comparison of variations in detected emissions from the S-EUT using vendor AF data and sphere-derived AF data.

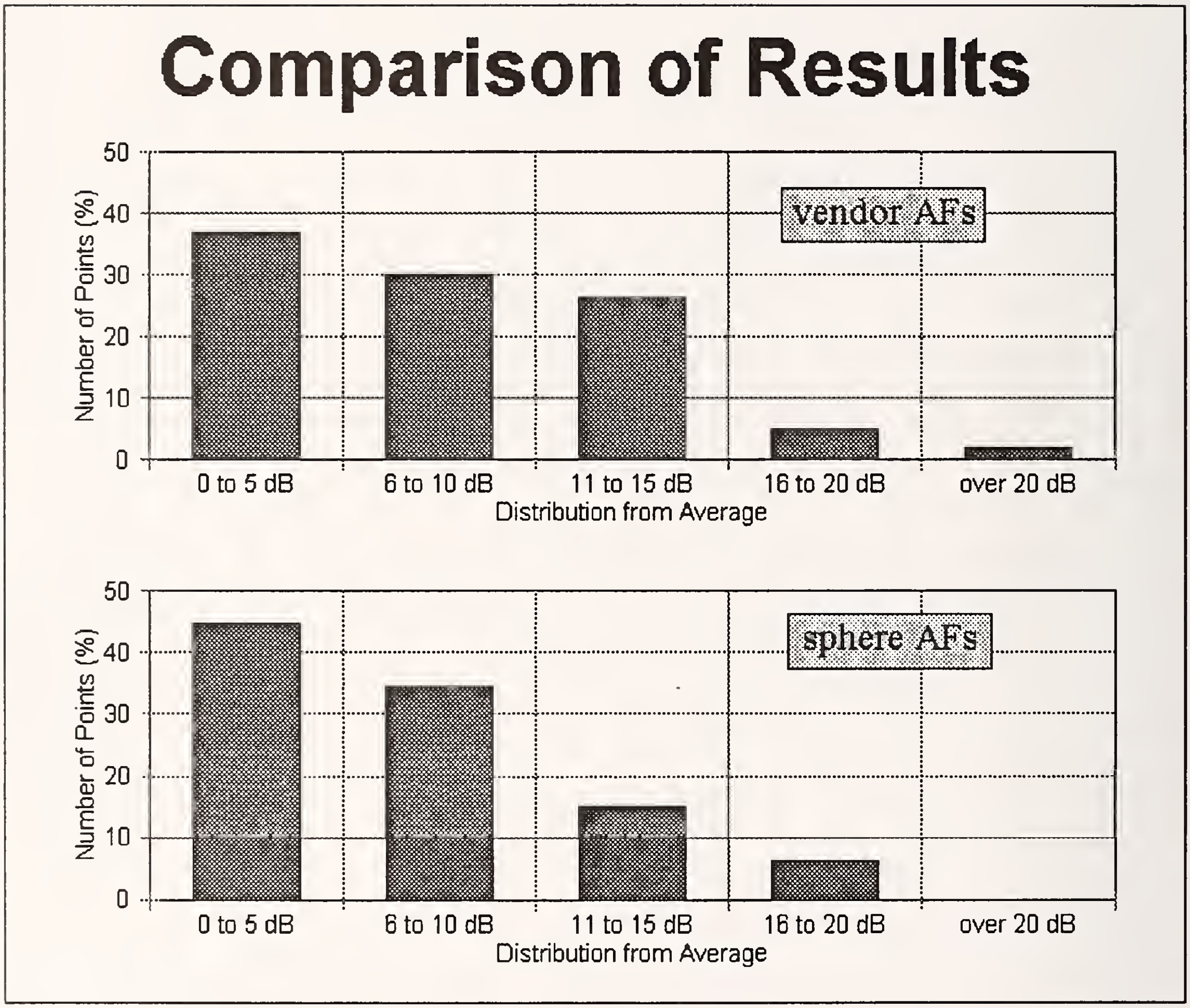

Figure 20. Comparison of distributions, about the average, for both vendor AF data and sphere-derived AF data on measured emissions from the S-EUT.

* U.S. GOVERNMENT PRINTING OFFICE 1996-0-774-018/40009

NIST Technical Publications

Periodical

Journal of Research of the National Institute of Standards and Technology—Reports NIST research and development in those disciplines of the physical and engineering sciences in which the Institute is active. These include physics, chemistry, engineering, mathematics, and computer sciences. Papers cover a broad range of subjects, with major emphasis on measurement methodology and the basic technology underlying standardization. Also included from time to time are survey articles on topics closely related to the Institute's technical and scientific programs. Issued six times a year.

Nonperiodicals

Monographs—Major contributions to the technical literature on various subjects related to the Institute's scientific and technical activities.

Handbooks—Recommended codes of engineering and industrial practice (including safety codes) developed in cooperation with interested industries, professional organizations, and regulatory bodies.

Special Publications—Include proceedings of conferences sponsored by NIST, NIST annual reports, and other special publications appropriate to this grouping such as wall charts, pocket cards, and bibliographies.

Applied Mathematics Series—Mathematical tables, manuals, and studies of special interest to physicists, engineers, chemists, biologists, mathematicians, computer programmers, and others engaged in scientific and technical work.

National Standard Reference Data Series—Provides quantitative data on the physical and chemical properties of materials, compiled from the world's literature and critically evaluated. Developed under a worldwide program coordinated by NIST under the authority of the National Standard Data Act (Public Law 90-396). NOTE: The Journal of Physical and Chemical Reference Data (JPCRD) is published bi-monthly for NIST by the American Chemical Society (ACS) and the American Institute of Physics (AIP). Subscriptions, reprints, and supplements are available from ACS, 1155 Sixteenth St., NW, Washington, DC 20056.

Building Science Series—Disseminates technical information developed at the Institute on building materials, components, systems, and whole structures. The series presents research results, test methods, and performance criteria related to the structural and environmental functions and the durability and safety characteristics of building elements and systems.

Technical Notes—Studies or reports which are complete in themselves but restrictive in their treatment of a subject. Analogous to monographs but not so comprehensive in scope or definitive in treatment of the subject area. Often serve as a vehicle for final reports of work performed at NIST under the sponsorship of other government agencies.

Voluntary Product Standards—Developed under procedures published by the Department of Commerce in Part 10, Title 15, of the Code of Federal Regulations. The standards establish nationally recognized requirements for products, and provide all concerned interests with a basis for common understanding of the characteristics of the products. NIST administers this program in support of the efforts of private-sector standardizing organizations.

Consumer Information Series—Practical information, based on NIST research and experience, covering areas of interest to the consumer. Easily understandable language and illustrations provide useful background knowledge for shopping in today's technological marketplace.

Order the **above** *NIST publications from: Superintendent of Documents, Government Printing Office, Washington, DC 20402.*

Order the **following** *NIST publications—FIPS and NISTIRs—from the National Technical Information Service, Springfield, VA 22161.*

Federal Information Processing Standards Publications (FIPS PUB)—Publications in this series collectively constitute the Federal Information Processing Standards Register. The Register serves as the official source of information in the Federal Government regarding standards issued by NIST pursuant to the Federal Property and Administrative Services Act of 1949 as amended, Public Law 89-306 (79 Stat. 1127), and as implemented by Executive Order 11717 (38 FR 12315, dated May 11, 1973) and Part 6 of Title 15 CFR (Code of Federal Regulations).

NIST Interagency Reports (NISTIR)—A special series of interim or final reports on work performed by NIST for outside sponsors (both government and non-government). In general, initial distribution is handled by the sponsor; public distribution is by the National Technical Information Service, Springfield, VA 22161, in paper copy or microfiche form.

U.S. Department of Commerce
National Institute of Standards and Technology
325 Broadway
Boulder, Colorado 80303-3328